Effects of Transverse Shear Deformations on the Free Vibration of Anisotropic Open Circular Cylindrical Shells

M. H. TOORANI and A. A. LAKIS

ÉCOLE POLYTECHNIQUE DE MONTRÉAL
Departement of Mechanical Engineering
Campus de l'Université de Montréal
C.P. 6079, Succ. Centre-Ville
Montréal (Québec)
H3C 3A7

April 1999

Dépot légal, April 1999
Bibliothèque nationale du Québec
Bibliothèque nationale du Canada

"Effects of Transverse Shear Deformations on the Free Vibration of Anisotropic Open Circular Cylindrical Shells" (**EPM/RT-99/4**)

M. H. Toorani , A. A. Lakis (Génie Mécanique)

Pour se procurer une copie de ce document, s'adresser au:

Service des Éditions
École Polytechnique de Montréal
Case postale 6079, Succursale Cnetre-Ville
Montréal (Québec) H3C 3A7
Téléphone: (514) 340-4473
Télécopie: (514) 340-3734

Compter 0,10 $ par page et ajouter 3,00 $ pour la couverture, les frais de poste et la manutention.
Régler en dollars canadiens par chèque ou manda-poste au nom de l'École Polytechnique de Montréal.

Nous n'honorons que les commandes accompagnées d'un paiement, sauf s'il y a eu entente préalable dans le cas d'établissements d'enseignement, de sociétés ou d'organismes canadiens.

NOMENCLATURE

A_i , B_i , C_i , …, J_i (i=1,2, …, 10) eqn (47) : defined by matrix components of [J]

A, B, C, D, E : defined by eqn(24)

A_{ij} : extensional stiffness eqn(20)

$A_{\alpha\beta}$:defined by eqn(21)

B_{ij} : bending-extensional coupling stiffness eqn(20)

$B_{\alpha\beta}$:defined by eqn(21)

D_{ij} :bending stiffness eqn(20)

f_i : coefficients of the characteristic equation (27)

h_i(i=1,2) : Scale factors eqn(2)

I_i : inertia moment

L : length of the shell

L_i : motion equations eqn(25)

m : axial mode number

$\overline{m}$: defined by $\frac{m\pi}{L}$

M_x, M_θ, $M_{x\theta}$, $M_{\theta x}$: the moment resultants

n : circumferential wave number

N_x, N_θ, $N_{x\theta}$, $N_{\theta x}$: the in-plane force resultants

P_{ij} : terms of elasticity matrix(i=1,... ,10 ; j=1,..., 10)

Q_{ij} : the elastic stiffness in the material coordinates eqn(10)

$\overline{Q}_{ij}$: the elastic stiffness in the global coordinates eqn(11)

Q_{xx}, $Q_{\theta\theta}$: the transverse force resultants

R : mean radius of the shell

t : thickness of the shell

u_1, u_2, w : the axial, circumferential and radial displacement respectively

U_m, V_m, W_m, β_{xm}, $\beta_{\theta m}$: amplitudes of u, v, w, β_x, and β_θ associated with m_{th} axial mode number

x : axial coordinate

α_i, β_i, γ_i and δ_i defined by eqn(29)

β_1 and β_2 : the rotations of tangents to the reference surface

η_i : complex roots of the characteristic eqn(27)

ε_i : deformation vector components

σ_i : stress vector component

θ : circumferential coordinate

ϕ_T : angle for the whole open shell

ω : natural frequency

Ω : non-dimensional frequency

ρ : density of the shell material

Liste of matrices

[A] : defined by eqn(35)

[B] : defined by equation(39)

{C}: vector for arbitrary constants

$\{f_i\}$: the internal forces acting at node ***i***

[G] : defined by eqn(47)

[H] : defined by eqn(26)

[J] : defined by eqn (39)

[k] : local stiffness matrix eqn(46)

[K] : global stiffness matrix eqn(50)

[m] : local mass matrix eqn(47)

[M] : global mass matrix eqn(50)

[N] : shape function matrix(37)

[QQ] : defined by eqn(38)

[R] : defined by eqn(42)

[S] : defined by eqn(44)

[T] : transformation matrix eqn(12)

$[T_m]$: defined by eqn(24)

$\{\delta_i\}$: degrees of freedom at node ***i***

$\{\delta_T\}$: degrees of freedom for total shell

List of Figures

Figure 15: Variation of non-dimensional natural frequency ($\Omega=\omega_o R^2(\rho/E_2)^{1/2}/t$) of anti-symmetric cross-ply ($0^o/90^o$) laminated cylindrical shells in conjunction with ***L/R*** and ***m*** variations.

Figure 16: Variation of non-dimensional natural frequency of cross-ply ($0^o/90^o$) cylindrical shells ($\Omega=\omega_o R^2(\rho/E_2)^{1/2}/t$) in terms of the ***L/R***'s variation(**n**=2, ***m***=1, ***L/t***=100).

Figure 17: Variation of non-dimensional natural frequency of cross-ply ($0^o/90^o$) cylindrical shells ($\Omega=\omega_o R^2(\rho/E_2)^{1/2}/t$) in terms of the ***L/R***'s variation(**n**=2, ***m***=5, ***L/t***=100).

Figure 18: Frequency distribution ($\Omega=\omega_o R^2(\rho/E_2)^{1/2}/t$) for various axial wave number (***m***) of symmetric cross-ply ($0^o/90^o/90^o/0^o$)laminated cylindrical shells(***L/t***=100,***n***=2).

Figure 19: Variation of non-dimensional frequency ($\Omega=\omega_o L^2(\rho/E_2)^{1/2}/t$) of symmetric cross-ply laminated cylindrical shells in conjunction with ***L/R*** and ***L/t*** variations.

Figure 20: Frequency distribution (Ω/Ω_o, $\Omega_o=\pi(G/\rho)^{1/2}/t$) for various axial wave number ($\lambda=m\pi R/L$) in terms of ***t/R***'s variation (***n***=1).

Figure 21: Frequency distribution (Ω/Ω_o, $\Omega_o=\pi(G/\rho)^{1/2}/t$) for various axial wave number ($\lambda=m\pi R/L$) in terms of ***t/R***'s variation (***n***=2).

Figure 22: Frequency distribution (Ω/Ω_o, $\Omega_o=\pi(G/\rho)^{1/2}/t$) for various axial wave number ($\lambda=m\pi R/L$) in terms of ***t/R***'s variation (***n***=3).

Figure 23: Frequency distribution (Ω/Ω_o, $\Omega_o=\pi(G/\rho)^{1/2}/t$) for various axial wave number ($\lambda=m\pi R/L$) in terms of ***t/R***'s variation (***n***=4).

Figure 24: Variation of non-dimensional natural frequency ($\Omega=\omega_o R^2(\rho/E_2)^{1/2}/t$) of a symmetric cross-ply open cylindrical shell for various ratios of ***L/R*** and ***m***.

Figure25: Frequency distribution ($\Omega=\omega_o R(\rho(1-\upsilon^2)/E)^{1/2}$) of an isotropic, open cylindrical shell in conjunction with ***L/R*** and ***m*** variations.

Résumé

Ce travail présente une approche raffinée pour l'analyse statique et dynamique des coques cylindriques minces élastiques et anisotropes laminés multicouches. L'analyse prend en compte les effets des déformations de cisaillement, de l'inertie de rotation aussi bien que de la courbure initiale. La méthode utilisée est une combinaison de la méthode des éléments finis hybrides et de la théorie des déformations de cisaillement des coque. La coque est divisée en plusieurs éléments finis de type coque cylindrique et les fonctions de déplacement sont dérivées de la théorie des coques cylindriques minces en coordonnés curvilignes orthogonaux. L'ensemble des matrices, les matrices de masse et de rigidité, qui décrivent leurs contributions relatives à l'équilibre sont déterminées par intégration analytique exacte. Cette théorie donne les déformations nulles pour le mouvement du corps rigide afin que les fonctions des déplacements basées sur cette théorie satisfont le critère de la convergence de la méthode des éléments finis. Cette théorie conduit à cinq équations différentielles du deuxième ordre, couplées et linéaires avec les coefficients constants. Elles sont résolues conjointement avec cinq conditions aux rives à chaque bord par une méthode des éléments finis hybrides. Les résultats obtenus concordent de façon raisonnable avec d'autres théories.

THE EFFECTS OF TRANSVERSE SHEAR DEFORMATION ON THE FREE VIBRATION OF ANISOTROPIC OPEN CIRCULAR CYLINDRICAL SHELLS

Abstract

This work presents a refined approach to the static and dynamic analysis of thin laminated anisotropic cylindrical shells by taking into account the shear deformation effect and rotary inertia as well as the initial curvature. The method used is a combination of hybrid finite element analysis and the shear deformation theory of shells. The shell is subdivided into cylindrical finite elements and the displacement functions are obtained using the shell equations based on orthogonal curvilinear coordinates. The set of matrices describing their relative contributions to equilibrium is determined by exact analytical integration. This theory gives zero strains for small rigid-body motions and therefore the displacement functions based on it satisfy the convergence criteria of the finite element method. This theory yields five coupled linear second-order differential equations with constant coefficients. They are solved in conjunction with five boundary conditions at each edge by a hybrid finite element method. Reasonable agreement is found with other theories.

*1. **Introduction***-Shells are widely used as structural elements in modern construction engineering, aircraft construction, ship building, and rocket construction, and in the nuclear, aerospace, aeronautical, petroleum and petrochemical industries. In order to minimise the number of problems which may arise during industrial use, it has become very important that the static and dynamic behavior of these structures, when subjected to different loads, be known and understood.

Many classical shell theories were developed originally for thin elastic shells, in both linear and non-linear cases, and are based on the Love-Kirchhoff assumptions which are as follows:
1) the shell is thin; 2) the displacements and rotation are small; 3) normals to the middle surface of shells before deformation remain normal after deformation, and 4) transverse normal stress is negligible. These assumptions could lead to gross errors in the prediction of transverse deflections, natural frequencies and buckling load due to the neglect of transverse shear deformations.

Surveys of various classical shell theories can be found in the works of Bert (1980), Reissner (1952) and Naghdi (1956). Papers covering the work of several researchers have been collected by Leissa (1973) into one excellent book. Elegant representations of Love's shell theory can be derived strictly by definitions from surface theory without reference to *3-D* relationships (Kraus 1967 & Ambartsumyan 1964).

There is an inconsistency in Love's original theory since all strains do not vanish for any rigid body motion. This inconsistency was solved by Sanders (1962) by redefining the force and moment resultants in such a way that the rigid body strain anomaly disappeared.
The thin shell assumption in Love's theory has been replaced by the less restrictive requirement on the thinness of the shell presented by Flügge, Lure and Byrne (Kraus 1967). Their theory also eliminated the

rigid body strain anomaly. Koiter (1960) discussed the significance of the Love's approximations and, based on an order of magnitude study, stated that refinements cannot be consistently made unless transverse deformation effects are included. Other prominent related theories include those of Novozhilov (1959).

The majority of the theories listed above have been applied to a shell so thin that all transverse deformation effects, transverse stresses and strains, can be neglected. These transverse effects become more pronounced as the shell becomes thicker relative to its in-plane dimensions, especially the transverse shear deformations (Koiter 1960). For this reason, classical theories can be grossly in error in the prediction of transverse deflections, buckling loads or natural frequencies.

These errors are even higher for plates and shells made of advanced composite materials like graphite-epoxy and boron-epoxy, where the ratio of elastic modulus to shear modulus is very large (e.g., of the order *25* to *40* instead of *2.6* for isotropic materials). The shear deformation effect plays a much more important role in reducing the effective stiffness of anisotropic laminated composite plates and shells.

Advanced composite materials are increasingly being used in a variety of industries because they have a high ratio of strength and stiffness to weight. For this reason, structural elements made up of these materials are being extensively used, e.g. in the aerospace, shipbuilding and petrochemical industries, etc., where complex shell configurations are common structural elements and offer unique advantages over those composed of isotropic materials.

In general, these materials are fiber-reinforced laminates, both symmetric and anti-symmetric, cross-ply and angle-ply, which consist of numerous layers each with different fiber orientations. Although the total laminate may exhibit orthotropic-like properties, each layer of the laminate is usually anisotropic.

Therefore, in order to gain insight into the actual stress and strain fields, the individual properties of each layer must be taken into account.

A number of theories for layered anisotropic shells exist in the literature. Many of these theories were developed for thin shells and are based on the Kirchhoff-Love hypothesis.

The transverse shear deformation effect on non-linear vibration and post-buckling behavior is significant, especially for the laminates with moderately significant thickness, a high circumferential wave number and greater number of layers. Study of this effect shows that it can become quite meaningful for some geometrical parameters, such as small radius to thickness or length to thickness ratios, as well as for shorter wavelengths or longer shells.

In addition to the transverse shear deformation, the initial curvature effect should be considered, as indicated by Voyiadjis and Shi (1991) for isotropic materials. The initial curvature effect is very important in making accurate predictions of stresses even in the central region. In the shell structure, the curvature of each parallel surface through the thickness of the shell is different. To consider the initial curvature effect, the term $1+z/R$ has to be included. The presence of curvature effectively increases the structural stiffness.

Hilderbrand, Reissner and Thomas (1949) were the first to make significant contributions by dispensing with all approximations of Love and assuming a three-term Taylor's series expansion for the displacement vector. Naghdi (1957) employed Reissner's (1950) mixed variational principle to develop a complete shell formulation similar to that of Hilderbrand et al. (1949), retaining two and three terms in the Taylor's series expansions for tangential and transverse displacement components, respectively.

Dong and Tso (1972) were perhaps the first to present a first order shear deformation theory,

retaining one and two terms in the Taylor's series for transverse and tangential displacement components respectively. The theory includes the effects of transverse shear deformation through the shell thickness, and thence they construct a laminated orthotropic shell theory. The parabolic shear strain distribution has been used by Bhimaraddi (1984) to analyze the linear vibrational behavior of isotropic cylindrical shells. The effects of transverse shear deformation and transverse isotropy as well as thermal expansion through the thickness of cylindrical shells were considered by Gulati and Essenberg (1967), Dong and his colleagues(1962), Hsu and Wang (1970).

Reddy (1984) extended Sanders' (1959) theory for simply supported cross-ply laminated shells assuming five degrees of freedom per node. The theory is based on a displacement field in which the displacements of the middle surface are expanded as cubic functions of the thickness coordinate, and the transverse displacement is assumed to be constant throughout the thickness. The Navier-type exact solutions for bending and natural vibration are presented for cylindrical and spherical shells under simply supported boundary conditions.

A survey of the analyses of multilayered composite shells using Reissner's mixed variational principle was carried out by Grigolyuk and Kulikov(1988). Noor and Peters (1987) presented an analysis of the free vibration of laminated anisotropic shells of revolution and the sensitivity of their response to anisotropic material coefficients. Noor and Peters' analytical formulation is based on a form of the Sanders-Budiansky shell theory, including the effects of both transverse shear deformation and the laminated anisotropic material response.

Ren (1989) presented an exact solution for simply supported laminated cross-ply circular cylindrical panels of infinite and finite length in the axial direction. Leissa et al. (1981) analysed the vibration of

cantilevered cylindrical panels by using the Ritz method, with algebraic polynomial functions for the displacements.

The static response of the axisymmetric problem of arbitrarily laminated, anisotropic cylindrical shells of finite length using three-dimensional elasticity equations was made by Jing and Zeng (1993). The closed cylinder is simply supported at both ends. The accuracy of a solution obtained by the finite element displacement formulation depends on whether the assumed functions accurately model the deformation modes of the given structure. To satisfy this criterion, Lakis and his group have developed a hybrid type of finite element, in which the displacement functions in the finite element method are derived from Sanders' (1959) classical shell theory.

This method has been applied with satisfactory results to the dynamic linear and non-linear analysis of cylindrical shells, both closed and open ((Lakis and Païdoussis (1971), (1972) & Lakis (1976) & Lakis and Doré (1978) & Lakis and Laveau (1991) & Lakis and Sinno (1992), Selmane and Lakis (1997), Toorani and Lakis (1999)), spherical (Lakis et al. 1989), conical (Lakis et al. 1992), isotropic and anisotropic, uniform and axially non-uniform shells, both empty and liquid-filled.

The main purpose of this work is to study the shear deformation, the rotary inertia and the initial curvature effects on the static and dynamic behavior of thin, anisotropic and non-uniform open and closed cylindrical shells. The flowing fluid effect on the natural frequencies of these shells will be the subject of a later work.

2. ***Basic Theory and Method***-Many classical shell theories were developed for thin elastic shells and a two-dimensional (*2-D*) theory, surface definitions, is used to approximate three-dimensional phenomena. These theories are based on the Love-Kirchhoff assumptions in which transverse shear strains and stresses

are frequently excluded. In this particular case, we use general *3-D* strain-displacement relations expressed in arbitrary orthogonal curvilinear coordinates to define the strain displacement relations which can easily be incorporated three-dimensionally.

This work is based on the following assumptions:

a) linear elastic behaviour of laminated anisotropic materials;

b) the shell is thin and therefore we can assume that the normal stress is negligible compared with stress tangential to the shell surface, and also that the transverse normal strain $\varepsilon_3 \cong 0$ because the transverse fibres of the shell are approximately inextensible;

c) *3-D* strain-displacement relations are expressed in arbitrary orthogonal curvilinear coordinates;

d) the transverse shear deformations, the rotary inertia and the initial curvature form the basis in the development of the governing equations;

Consider the infinitesimal line segment **MN**, which is infinitesimally near another one, of length ***ds*** embedded in a differential volume element **B** before transformation. As a result of the deformation **M** and **N** are displaced to **M*** and **N*** respectively, by the displacement vector ***u*** (Figure1). The change in length of the element **MN** can be expressed by:

$$(ds*)^2 - (ds)^2 = 2\gamma_{ij} dy_i dy_j \qquad (1)$$

where the quantity $[(ds^*)^2 - (ds)^2]$ is an invariant and $\gamma_{ij} = \gamma_{ji}$ is a second-rank symmetric tensor called Green's strain tensor and y_i are the orthogonal curvilinear coordinates of the undeformed system. The physical strains, ε_{ij}, are defined as [Saada 1993]:

$$\varepsilon_{ij} = \frac{\gamma_{ij}}{h_i h_j} \tag{2}$$

where, the h_i are called scale factors and defined by $G_{ij} = h_i^2$ (no sum), and G_{ij} is a metric tensor which links two coordinate systems. The γ_{ij} are given in the Appendix, where the u_i are the coordinates of the displacement vectors, u. For rigid body motion, the elongations ε_{ii} (no sum) and the shears $\varepsilon_{ij}(i \neq j)$ are identically zero, and therefore there are no theoretical limitations.

The geometrical scale factor quantities (h_i's) must be defined to use the strain displacement relations for the shells. We now consider a shell geometry that can be described by orthogonal curvilinear middle surface coordinates, α_1 and α_2, surface normal ξ and radii of curvature, R_1 and R_2 as shown in (Figure 2). For this geometry, the scale factor terms are defined below:

$$h_1 = \sqrt{E}(1 - \xi/R_1),\ h_2 = \sqrt{G}(1 - \xi/R_2),\ h_3 = 1 \tag{3}$$

where **E** and **G** are called the first fundamental magnitudes and are related to the elements of the surface metric [Kraus 1967].

2.1 Kinematics - We consider the following kinematic relations for the arbitrary shell described by orthogonal curvilinear coordinates.

$$\begin{aligned} u(\alpha_1,\alpha_2,\xi) &= (1 + \frac{\xi}{R_1})u_1(\alpha_1,\alpha_2) + \xi\beta_1(\alpha_1,\alpha_2) \\ v(\alpha_1,\alpha_2,\xi) &= (1 + \frac{\xi}{R_2})u_2(\alpha_1,\alpha_2) + \xi\beta_2(\alpha_1,\alpha_2) \\ w(\alpha_1,\alpha_2,\xi) &= w_1(\alpha_1,\alpha_2) \end{aligned} \tag{4}$$

where the five degrees of freedom, u_1, u_2, w, β_1 and β_2 are functions of the in-plane coordinates α_1 and α_2 in which u_1, u_2 and w are, respectively, the axial, circumferential and radial displacements, and β_α (α=1,2) are rotations of tangents to the reference surface oriented along parametric lines α_1 and α_2 respectively.

These theories relax the Kirchhoff-Love hypothesis which requires normals to the mid-plane to remain normal throughout deformation. If we substitute equations (4) into equations (2), we obtain the following strain-displacement relations for cylindrical shells:

$$\begin{aligned} \varepsilon_x &= \varepsilon^o{}_x + \xi\kappa_x \\ \varepsilon_\theta &= \varepsilon^o{}_\theta + \xi\kappa_\theta \\ \gamma_{x\theta} &= (\gamma^o{}_x + \gamma^o{}_\theta) + \xi(\tau_x + \tau_\theta) \\ \gamma_{xn} &= \mu^o{}_x = 2\varepsilon_{xn} \\ \gamma_{\theta n} &= \mu^o{}_\theta = 2\varepsilon_{\theta n} \end{aligned} \tag{5}$$

Where:

$$\begin{aligned} \varepsilon^o{}_x &= \frac{\partial U_x}{\partial x} \quad ; \quad \kappa_x = \frac{\partial \beta_x}{\partial x} \\ \varepsilon^o{}_\theta &= \frac{1}{R}\frac{\partial U_\theta}{\partial \theta} + \frac{W}{R} \quad ; \quad \kappa_\theta = \frac{1}{R}\frac{\partial \beta_\theta}{\partial \theta} \\ \gamma^o{}_x &= \frac{\partial U_\theta}{\partial x} \quad ; \quad \tau_x = \frac{\partial \beta_\theta}{\partial x} + \frac{1}{2R}\frac{\partial U_\theta}{\partial x} \\ \gamma^o{}_\theta &= \frac{1}{R}\frac{\partial U_x}{\partial \theta} \quad ; \quad \tau_\theta = \frac{1}{R}\frac{\partial \beta_x}{\partial \theta} - \frac{1}{2R^2}\frac{\partial U_x}{\partial \theta} \\ \mu^o{}_x &= \frac{\partial W}{\partial x} + \beta_x \quad ; \quad \mu^o{}_\theta = \frac{1}{R}\frac{\partial W}{\partial \theta} - \frac{U_\theta}{R} + \beta_\theta \end{aligned} \tag{6}$$

Where $\varepsilon^o{}_i$; $\gamma^o{}_i$; κ_i; τ_i and $\mu^o{}_i$ are, respectively, the normal and in-plane shear strain, the change in the curvature and torsion of the reference surface, and the shear strain components. The interested reader is

referred to [Toorani and Lakis 1999].

2.2 Constitutive Relations The relationship between the stress and strain vectors (Hook's law) is:

$$\{\sigma\} = [P]\{\varepsilon\} \tag{7}$$

The constitutive equation of the K_{th} lamina (for a lamina of fibre-reinforced composite material) in the lamina reference axes $(1,2,3)$ can be written as follows (Figure 3):

$$\begin{Bmatrix} \sigma_1 \\ \sigma_2 \\ \sigma_3 \\ \tau_{23} \\ \tau_{13} \\ \tau_{12} \end{Bmatrix} = \begin{bmatrix} Q_{11} & Q_{12} & Q_{13} & 0 & 0 & 0 \\ Q_{21} & Q_{22} & Q_{23} & 0 & 0 & 0 \\ Q_{31} & Q_{32} & Q_{33} & 0 & 0 & 0 \\ 0 & 0 & 0 & 2Q_{44} & 0 & 0 \\ 0 & 0 & 0 & 0 & 2Q_{55} & 0 \\ 0 & 0 & 0 & 0 & 0 & 2Q_{66} \end{bmatrix} \begin{Bmatrix} \varepsilon_1 \\ \varepsilon_2 \\ \varepsilon_3 \\ \varepsilon_{23} \\ \varepsilon_{13} \\ \varepsilon_{12} \end{Bmatrix} \tag{8}$$

$$\tau_{23} = \frac{1}{2} G_{23} \varepsilon_{23} \ , \ \tau_{13} = \frac{1}{2} G_{13} \varepsilon_{13} \ , \ \tau_{12} = \frac{1}{2} G_{12} \varepsilon_{12} \tag{9}$$

The [Q] matrix denotes the elastic stiffness in the material coordinates (local axes). The Q_{ij}'s elements are defined as follows:

$$\begin{aligned} Q_{11} &= E_{11}(1 - \nu_{23}\nu_{32})/\Delta \ ; \ Q_{44} = G_{23} \\ Q_{22} &= E_{22}(1 - \nu_{31}\nu_{13})/\Delta \ ; \ Q_{55} = G_{13} \\ Q_{33} &= E_{11}(1 - \nu_{12}\nu_{21})/\Delta \ ; \ Q_{66} = G_{12} \\ Q_{12} &= (\nu_{21} + \nu_{31}\nu_{23})E_{11}/\Delta = (\nu_{12} + \nu_{32}\nu_{13})E_{22}/\Delta \\ Q_{13} &= (\nu_{31} + \nu_{21}\nu_{32})E_{11}/\Delta = (\nu_{13} + \nu_{12}\nu_{23})E_{33}/\Delta \\ Q_{23} &= (\nu_{32} + \nu_{12}\nu_{31})E_{22}/\Delta = (\nu_{23} + \nu_{21}\nu_{13})E_{33}/\Delta \\ \Delta &= 1 - \nu_{12}\nu_{21} - \nu_{23}\nu_{32} - \nu_{31}\nu_{13} - 2\nu_{21}\nu_{32}\nu_{13} \end{aligned} \tag{10}$$

where E_{ij}, G_{ij} and v_{ij} are, respectively, Young's moduli of elasticity in the principal directions, rigidity moduli which characterize the change of angle between the principal directions, and the Poisson ratios which characterize the transverse contraction (expansion) under tension (compression) in the directions of the coordinate axes.

The stress-strain relations of the K_{th} lamina in the laminate coordinate axes (x,y,z global coordinates) can be written as (Figure 4a):

$$\{\bar{\sigma}\} = \begin{Bmatrix} \sigma_x \\ \sigma_\theta \\ \sigma_n \\ \tau_{\theta n} \\ \tau_{xn} \\ \tau_{x\theta} \end{Bmatrix} = \begin{bmatrix} \overline{Q_{11}} & \overline{Q_{12}} & \overline{Q_{13}} & 0 & 0 & 2\overline{Q_{16}} \\ \overline{Q_{21}} & \overline{Q_{22}} & \overline{Q_{26}} & 0 & 0 & 2\overline{Q_{26}} \\ \overline{Q_{31}} & \overline{Q_{32}} & \overline{Q_{33}} & 0 & 0 & 2\overline{Q_{36}} \\ 0 & 0 & 0 & 2\overline{Q_{44}} & 2\overline{Q_{45}} & 0 \\ 0 & 0 & 0 & 2\overline{Q_{54}} & 2\overline{Q_{55}} & 0 \\ \overline{Q_{16}} & \overline{Q_{26}} & \overline{Q_{36}} & 0 & 0 & 2\overline{Q_{66}} \end{bmatrix} \begin{Bmatrix} \varepsilon_x \\ \varepsilon_\theta \\ \varepsilon_n \\ \gamma_{\theta n} \\ \gamma_{xn} \\ \gamma_{x\theta} \end{Bmatrix} \tag{11}$$

where :

$$[\bar{Q}] = [T]^{-1}[Q][T] \tag{12}$$

The transformation matrix [T] is defined by:

$$[T] = \begin{bmatrix} m^2 & n^2 & 0 & 0 & 0 & 2mn \\ n^2 & m^2 & 0 & 0 & 0 & -2mn \\ 0 & 0 & 1 & 0 & 0 & 0 \\ 0 & 0 & 0 & m & -n & 0 \\ 0 & 0 & 0 & n & m & 0 \\ -mn & mn & 0 & 0 & 0 & (m^2-n^2) \end{bmatrix} \tag{13}$$

where: $m \equiv \cos\alpha$, $n \equiv \sin\alpha$

The orientation angle θ is measured counter-clockwise from the x-axis to the 1-axis (Figure 4b). The

$[\overline{Q}]$'s elements are defined as follows:

$$\overline{Q'_{ij}} \textit{elements:}$$

$$\overline{Q_{11}}=Q_{11}m^4+2(Q_{12}+2Q_{66})m^2n^2+Q_{22}n^4 \quad ; \quad \overline{Q_{22}}=Q_{11}n^4+2(Q_{12}+2Q_{66})m^2n^2+Q_{22}m^4$$

$$\overline{Q_{12}}=(Q_{11}+Q_{22}-4Q_{66})m^2n^2+Q_{12}(m^4+n^4) \quad ; \quad \overline{Q_{23}}=Q_{13}n^2+Q_{23}m^2$$

$$\overline{Q_{13}}=Q_{13}m^2+Q_{23}n^2 \quad ; \quad \overline{Q_{26}}=-m^3nQ_{22}+mn^3Q_{11}+mn(m^2-n^2)(Q_{12}+2Q_{66})$$

$$\overline{Q_{16}}=-mn^3Q_{22}+m^3nQ_{11}-mn(m^2-n^2)(Q_{12}+2Q_{66}) \quad , \quad \overline{Q_{66}}=(Q_{11}+Q_{22}-2Q_{12})m^2n^2+Q_{66}(m^2-n^2)^2 \qquad (14)$$

$$\overline{Q_{33}}=Q_{33}$$

$$\overline{Q_{36}}=(Q_{13}-Q_{23})mn \quad ; \quad \overline{Q_{45}}=(Q_{55}-Q_{44})mn$$

$$\overline{Q_{44}}=Q_{44}m^2+Q_{55}n^2 \quad ; \quad \overline{Q_{55}}=Q_{55}m^2+Q_{44}n^2$$

3. *Fundamental equations for open cylindrical shells*

3.1 ***The Equations of Motion-*** Whenever a new theory based on assumed displacements is developed, the governing equilibrium equations should be derived by using one of the existing methods. We use the virtual displacements principle. The circular cylindrical shell geometry and the differential element studied, as well as the coordinates used, are shown in (Figure 5). The equations of motion are:

$$\frac{\partial N_{xx}}{\partial x}+\frac{1}{R}\frac{\partial N_{\theta x}}{\partial \theta}-\frac{1}{R^2}\frac{\partial M_{\theta x}}{\partial \theta}+q_x=I_1\ddot{u}_x+I_2\ddot{\beta}_x$$

$$\frac{\partial N_{x\theta}}{\partial x}+\frac{1}{R}\frac{\partial N_{\theta\theta}}{\partial \theta}+\frac{Q_{\theta\theta}}{R}+\frac{1}{2R}\frac{\partial M_{x\theta}}{\partial x}+q_\theta=I_1\ddot{u}_\theta+I_2\ddot{\beta}_\theta$$

$$\frac{\partial Q_{xx}}{\partial x}+\frac{1}{R}\frac{\partial Q_{\theta\theta}}{\partial \theta}-\frac{N_{\theta\theta}}{R}+q_n=I_1\ddot{w} \qquad (15)$$

$$\frac{\partial M_{xx}}{\partial x}+\frac{1}{R}\frac{\partial M_{\theta x}}{\partial \theta}-Q_{xx}=I_2\ddot{u}_x+I_3\ddot{\beta}_x$$

$$\frac{1}{R}\frac{\partial M_{\theta\theta}}{\partial \theta}+\frac{\partial M_{x\theta}}{\partial x}-Q_{\theta\theta}=I_2\ddot{u}_\theta+I_3\ddot{\beta}_\theta$$

where :

$$I_1, I_2, I_3 = \sum_{k=1}^{N} \int_{h_k}^{h_{k-1}} \rho^{(k)}(1, \xi, \xi^2) d\xi \tag{16}$$

where I_i, $\rho^{(k)}$ and ξ are, respectively, the inertia moments, the density of the lamina material and the thickness coordinate.

It can be seen that there are five independent boundary conditions to be applied at given edges. The transverse shear deformations do not vanish in the present theory and, therefore, the βi cannot be expressed in terms of U_i and W. The transverse shear theory recommended here leads to no strains during rigid body motion.

3.2 <u>The stress resultants and stress couples</u> The stress resultants and stress couples are given by:

$$\begin{Bmatrix} N_x \\ N_{x\theta} \\ Q_x \end{Bmatrix} = \int_{\xi} \begin{Bmatrix} \sigma_x \\ \tau_{x\theta} \\ \tau_{xn} \end{Bmatrix} (1+\xi/R_\theta)\, d\xi \quad ; \quad \begin{Bmatrix} N_\theta \\ N_{\theta x} \\ Q_\theta \end{Bmatrix} = \int_{\xi} \begin{Bmatrix} \sigma_\theta \\ \tau_{\theta x} \\ \tau_{\theta n} \end{Bmatrix} (1+\xi/R_\varphi)\, d\xi$$

$$\begin{Bmatrix} M_x \\ M_{x\theta} \end{Bmatrix} = \int_{\xi} \begin{Bmatrix} \sigma_x \\ \tau_{x\theta} \end{Bmatrix} (1+\xi/R_\theta)\, d\xi \quad ; \quad \begin{Bmatrix} M_\theta \\ M_{\theta x} \end{Bmatrix} = \int_{\xi} \begin{Bmatrix} \sigma_\theta \\ \tau_{\theta x} \end{Bmatrix} (1+\xi/R_\varphi)\, d\xi \tag{17}$$

The quantities (N_{xx}, $N_{\theta\theta}$, $N_{x\theta}$, $N_{\theta x}$) are called the *in-plane force resultants*, (M_{xx}, $M_{\theta\theta}$, $M_{x\theta}$, $M_{\theta x}$) are called the *moment resultants* and (Q_{xx}, $Q_{\theta\theta}$) denote the *transverse force resultants*. We notice, in equations (17), that the symmetry of the stress tensor ($\tau_{x\theta} = \tau_{\theta x}$) does not necessarily imply that $N_{x\theta}$ and $N_{\theta x}$ are equal or that $M_{x\theta}$ and $M_{\theta x}$ are equal except in the case of a spherical shell, a flat plate or a thin shell of any shape.

3.3 ***The Constitutive Equations*** The stress resultants and stress couples that correspond to the remaining stress are given by equations (17), so, using equations (5), (11) and (17) we have:

$$\begin{Bmatrix} N_{xx} \\ N_{x\theta} \\ N_{\theta\theta} \\ N_{\theta x} \end{Bmatrix} = \underset{(4\times4)}{\begin{bmatrix} A_{ij}+B_{ij}/R & A_{ij}+B_{ij}/R \\ A_{ij} & A_{ij} \end{bmatrix}} \begin{Bmatrix} \varepsilon^{o}_{x} \\ \gamma^{o}_{x} \\ \varepsilon^{o}_{\theta} \\ \gamma^{o}_{\theta} \end{Bmatrix} + \underset{(4\times4)}{\begin{bmatrix} B_{ij}+D_{ij}/R & B_{ij}+D_{ij}/R \\ B_{ij} & B_{ij} \end{bmatrix}} \begin{Bmatrix} \kappa_{x} \\ \tau_{x} \\ \kappa_{\theta} \\ \tau_{\theta} \end{Bmatrix} \qquad i,j=1,6,2,6 \tag{18}$$

$$\begin{Bmatrix} M_{xx} \\ M_{x\theta} \\ M_{\theta\theta} \\ M_{\theta x} \end{Bmatrix} = \underset{(4\times4)}{\begin{bmatrix} B_{ij}+D_{ij}/R & B_{ij}+D_{ij}/R \\ B_{ij} & B_{ij} \end{bmatrix}} \begin{Bmatrix} \varepsilon^{o}_{x} \\ \gamma^{o}_{x} \\ \varepsilon^{o}_{\theta} \\ \gamma^{o}_{\theta} \end{Bmatrix} + \underset{(4\times4)}{\begin{bmatrix} D_{ij}+E_{ij}/R & D_{ij}+E_{ij}/R \\ D_{ij} & D_{ij} \end{bmatrix}} \begin{Bmatrix} \kappa_{x} \\ \tau_{x} \\ \kappa_{\theta} \\ \tau_{\theta} \end{Bmatrix} \qquad i,j=1,6,2,6 \tag{19}$$

Note : $Nx\theta \neq N\theta x$ and $Mx\theta \neq M\theta x$

where:

$$\begin{aligned} A_{ij} &= \sum_{k=1}^{N} (\overline{Q_{ij}})_k (h_k - h_{k-1}) \\ B_{ij} &= \frac{1}{2}\sum_{k=1}^{N} (\overline{Q_{ij}})_k (h^2{}_k - h^2{}_{k-1}) \qquad i,j=1,6,2,6 \\ D_{ij} &= \frac{1}{3}\sum_{k=1}^{N} (\overline{Q_{ij}})_k (h^3{}_k - h^3{}_{k-1}) \\ E_{ij} &= \frac{1}{4}\sum_{k=1}^{N} (\overline{Q_{ij}})_k (h_k{}^4 - h^4{}_{k-1}) \end{aligned} \tag{20}$$

[A] and *[D]* are the extensional and flexural stiffness matrices, which relate the in-plane stress resultant (N) to the mid-surface strains (εo) and the stress couples (M) to the curvatures (κo).

[B] is the bending-stretching coupling matrix. It should be noted that a laminated structure can have the bending-stretching coupling even if all laminae are isotropic. All of the B_{ij} components can be equal to zero

if and only if the structure is exactly symmetrical about its middle surface.

We also have:

$$\begin{Bmatrix} Q_{xx} \\ Q_{\theta\theta} \end{Bmatrix} = \begin{bmatrix} 2(A_{55}+B_{55}/R) & 2(A_{54}+B_{54}/R) \\ 2A_{45} & 2A_{44} \end{bmatrix} \begin{Bmatrix} \mu^{o}_{x} \\ \mu^{o}_{\theta} \end{Bmatrix} \tag{21}$$

where:

$$\begin{aligned} A_{\alpha\beta} &= \sum_{k=1}^{N} (\overline{Q_{\alpha\beta}})_k (h_k - h_{k-1}) \\ B_{\alpha\beta} &= \frac{1}{2} \sum_{k=1}^{N} (\overline{Q_{\alpha\beta}})_k (h^2{}_k - h^2{}_{k-1}) \end{aligned} \qquad \alpha,\beta = 4,5 \tag{22}$$

Finally:

$$\begin{Bmatrix} N_{xx} \\ N_{x\theta} \\ Q_{xx} \\ N_{\theta\theta} \\ N_{\theta x} \\ Q_{\theta\theta} \\ M_{xx} \\ M_{x\theta} \\ M_{\theta\theta} \\ M_{\theta x} \end{Bmatrix} = [P] \begin{Bmatrix} \varepsilon^{o}_{x} \\ \gamma^{o}_{x} \\ \mu^{o}_{x} \\ \varepsilon^{o}_{\theta} \\ \gamma^{o}_{\theta} \\ \mu^{o}_{\theta} \\ \kappa_x \\ \tau_x \\ \kappa_\theta \\ \tau_\theta \end{Bmatrix} = [P]_{(10\times10)} \begin{Bmatrix} \frac{\partial u_x}{\partial x} \\ \frac{\partial u_\theta}{\partial x} \\ \frac{\partial w}{\partial x} + \beta_x \\ \frac{1}{R}\frac{\partial u_\theta}{\partial \theta} + \frac{w}{R} \\ \frac{1}{R}\frac{\partial u_x}{\partial \theta} \\ \frac{1}{R}\frac{\partial w}{\partial \theta} - \frac{u_\theta}{R} + \beta_\theta \\ \frac{\partial \beta_x}{\partial x} \\ \frac{\partial \beta_\theta}{\partial x} + \frac{1}{2R}\frac{\partial u_\theta}{\partial x} \\ \frac{1}{R}\frac{\partial \beta_\theta}{\partial \theta} \\ \frac{1}{R}\frac{\partial \beta_x}{\partial \theta} - \frac{1}{2R^2}\frac{\partial u_x}{\partial \theta} \end{Bmatrix}_{(10\times1)} \tag{23}$$

The ε^{o}_{x}, γ^{o}_{x} ..., and τ_θ were given earlier in equation (6). The elasticity matrix [P] given in equation

(23) can be applied to shells consisting of a single or an arbitrary number of isotropic, quasi-isotropic and orthotropic layers. In the case of an arbitrary number of orthotropic layers, we assume that these layers function concurrently without slippage. The *[P]* matrix is given in the Appendix.

4. The Displacement Functions-In the continuum, we express $u, v, w, \beta x$ and $\beta\theta$ of the mean surface of the shell by:

$$\begin{Bmatrix} U(x,\theta) \\ V(x,\theta) \\ W(x,\theta) \\ \beta_x(x,\theta) \\ \beta_\theta(x,\theta) \end{Bmatrix} = \sum_{i=1}^{10} \begin{bmatrix} Cos\bar{m}x & 0 & 0 & 0 & 0 \\ 0 & Sin\bar{m}x & 0 & 0 & 0 \\ 0 & 0 & Sin\bar{m}x & 0 & 0 \\ 0 & 0 & 0 & Cos\bar{m}x & 0 \\ 0 & 0 & 0 & 0 & Sin\bar{m}x \end{bmatrix} \begin{Bmatrix} u_i(\theta) \\ v_i(\theta) \\ w_i(\theta) \\ \beta_{x_i}(\theta) \\ \beta_{\theta_i}(\theta) \end{Bmatrix} = \sum_{i=1}^{10} [T_1] \begin{Bmatrix} A_i e^{\eta_i \beta} \\ B_i e^{\eta_i \beta} \\ C_i e^{\eta_i \beta} \\ D_i e^{\eta_i \beta} \\ E_i e^{\eta_i \beta} \end{Bmatrix} \tag{24}$$

where:

$$\bar{m} = \frac{m\pi}{L}$$

where ***m*** is the longitudinal wave number. We substitute equations (23) into the equations of motion (15), and obtain the five linear differential operators ***Li***(i=1,2,...,5). These equations, in which the shear deformation effects and inertia terms as well as the initial curvature are included, are given in the Appendix.

$$\begin{aligned} &L_1(U,V,W,\beta_x,\beta_\theta,\overline{P_{ij}})=0. \\ &L_2(U,V,W,\beta_x,\beta_\theta,\overline{P_{ij}})=0. \\ &L_3(U,V,W,\beta_x,\beta_\theta,\overline{P_{ij}})=0. \\ &L_4(U,V,W,\beta_x,\beta_\theta,\overline{P_{ij}})=0. \\ &L_5(U,V,W,\beta_x,\beta_\theta,\overline{P_{ij}})=0. \end{aligned} \tag{25}$$

We substitute equations (24) into the equations of motion (25), and obtain:

$$[H]_{(5\times5)}\begin{Bmatrix}A\\B\\C\\D\\E\end{Bmatrix}_{(5\times1)}=\begin{Bmatrix}0\\0\\0\\0\\0\end{Bmatrix}_{(5\times1)} \tag{26}$$

For the non-trivial solution, the determinant of matrix *[H]* must vanish. This brings us to the following polynomial equation (characteristic equation):

$$Det([H])=f_{10}\eta^{10}+f_8\eta^8+f_6\eta^6+f_4\eta^4+f_2\eta^2+f_0 \tag{27}$$

Where f_i (i=0 to 10) are the coefficients of the determinant of the equation of motion *[H]* given in the Appendix. Each root of this equation yields a solution to the equation of motion. The complete solution is obtained by the sum of all ten independent solutions with the constants A_p, B_p, C_p, D_p and E_p, so that:

$$\begin{aligned}u(x)&=A_p e^{\eta\theta}\\ v(x)&=B_p e^{\eta\theta}\\ w(x)&=C_p e^{\eta\theta}\\ \beta_x(x)&=D_p e^{\eta\theta}\\ \beta_\theta(x)&=E_p e^{\eta\theta}\end{aligned}\qquad p=1,...,10 \tag{28}$$

The constants A_p, B_p, C_p, D_p and E_p are dependent; we can therefore express these constants as a function of C_p:

$$A_p=\alpha_p C_p\ ,B_p=\beta_p C_p\ ,D_p=\gamma_p C_p\ ,E_p=\delta_p C_p \qquad (p=1,2,..,10) \tag{29}$$

The values of α_p,β_p,γ_p and δ_p can be obtained from the following relations:

$$\begin{bmatrix} H_{11} & H_{12} & H_{14} & H_{15} \\ H_{21} & H_{22} & H_{24} & H_{25} \\ H_{41} & H_{42} & H_{44} & H_{45} \\ H_{51} & H_{52} & H_{54} & H_{55} \end{bmatrix} \begin{Bmatrix} \alpha_p \\ \beta_p \\ \gamma_p \\ \delta_p \end{Bmatrix} = \begin{Bmatrix} -H_{13} \\ -H_{23} \\ -H_{43} \\ -H_{53} \end{Bmatrix} \tag{30}$$

The elements of matrix *[H]* are given in the Appendix. The displacements $U(x, \theta), V(x, \theta)$ and $W(x, \theta)$ as well as $\beta_x(x,\theta)$ and $\beta_\theta(x,\theta)$ can then be expressed in conjunction with the ten ***Cp*** constants only. We then have:

$$\begin{Bmatrix} U(x,\theta) \\ V(x,\theta) \\ W(x,\theta) \\ \beta_x(x,\theta) \\ \beta_\theta(x,\theta) \end{Bmatrix} = [T_1]_{(5\times5)} [\bar{R}]_{(5\times10)} \{C\}_{(10\times1)} \tag{31}$$

where $[\bar{R}]$'s matrix is given in Appendix ???, and $\{C\}$ is the tenth order vector of the constants' ***Cp***.

$$\{C\} = \{C_1, \ldots, C_{10}\}^T \tag{32}$$

Setting $[\bar{R}]$ =[LL] [X], equation (31) becomes:

$$\begin{Bmatrix} U(x,\theta) \\ V(x,\theta) \\ W(x,\theta) \\ \beta_x(x,\theta) \\ \beta_\theta(x,\theta) \end{Bmatrix} = \underset{(5\times5)}{[T_1]} \underset{(5\times10)}{[LL]} \underset{(10\times10)}{[X]} \underset{(10\times1)}{\{C\}} \tag{33}$$

where the [LL] and [X] matrices are given in the Appendix. To determine the ten ***Cp*** constants, it is necessary to formulate ten boundary conditions for the finite elements, the axial, tangential and radial

displacements as well as the rotations will be specified for each node. The degree of freedom at node ***i*** can be defined by the vector:

$$\{\delta_i\}=\{u_i \;\; v_i \;\; w_i \;\; \alpha_i \;\; \beta_i\}^T \tag{34}$$

The elements, which have two nodes and ten degrees of freedom, will have (***i, θ=0***) and (***j, θ=φ***) as nodal displacements at the boundaries:

$$\begin{Bmatrix}\delta_i\\ \delta_j\end{Bmatrix}=\{U_i \;\; V_i \;\; W_i \;\; \beta_{x_i} \;\; \beta_{\theta_i} \;\; U_j \;\; V_j \;\; W_j \;\; \beta_{x_j} \;\; \beta_{\theta_j}\}^T=[A]_{(10\times10)}\;\{C\}_{(10\times1)} \tag{35}$$

Simply Supported : $v = w = \varphi_2 = N_1 = M_1 = 0$.

Clamped : $u = v = w = \varphi_1 = \varphi_2 = 0$.

Free : $N_1 = M_1 = Q_1 = N_6 = M_6 = 0$.

where the [A] matrix terms are obtained from matrix [R] by successively setting $\theta=0$ and $\theta=\varphi$. Multiplying equation (35) by $[A]^{-1}$ we obtain:

$$\{C\}=[A]^{-1}\begin{Bmatrix}\delta_i\\ \delta_j\end{Bmatrix} \tag{36}$$

where [A] is given in the Appendix. Substituting for equation (33) we get:

$$\begin{Bmatrix}U(x,\theta)\\ V(x,\theta)\\ W(x,\theta)\\ \beta_x(x,\theta)\\ \beta_\theta(x,\theta)\end{Bmatrix}=[T_1][LL][X][A]^{-1}\begin{Bmatrix}\delta_i\\ \delta_j\end{Bmatrix}=[N]\begin{Bmatrix}\delta_i\\ \delta_j\end{Bmatrix} \tag{37}$$

These equations determine the displacement functions.

5. Determination of Mass and Stiffness Matrices for an Element - The strain vector may be found by using equations (5) and (37):

$$\{\varepsilon\} = \begin{bmatrix} [T_1] & 0 \\ 0 & [T_1] \end{bmatrix} [QQ][A]^{-1} \begin{Bmatrix} \delta_i \\ \delta_j \end{Bmatrix} \tag{38}$$

Assume that [QQ]=[J][X], therefore equation (38) becomes:

$$\{\varepsilon\} = [T]_{(10\times10)}[J]_{(10\times10)}[X]_{(10\times10)}[A]^{-1}{}_{(10\times10)} \begin{Bmatrix} \delta_i \\ \delta_j \end{Bmatrix}_{(10\times1)} = [BB] \begin{Bmatrix} \delta_i \\ \delta_j \end{Bmatrix} \tag{39}$$

The matrices of [T] and [Q] are given in Appendix ???. Combination equations (7) and (39), the stress-strain relations, can be written as:

$$\{\sigma\} = [P][BB] \begin{Bmatrix} \delta_i \\ \delta_j \end{Bmatrix} \tag{40}$$

The mass matrix can be expressed as:

$$[m] = \rho t \int_0^L \int_0^{\varphi} [N]^T [N] \, dA \tag{41}$$

Where $dA=Rdx\,d\theta$. Or

$$[m]=\rho t\int_0^L\int_0^{\varphi}[A^{-1}]^T\left\{[\bar{R}]^T[T_1]^T[T_1][\bar{R}]\right\}[A^{-1}]r\,dx\,d\theta \tag{42}$$

Using equation (37), equation (42), after integration with respect to x and θ, over the interval, becomes:

$$[m]=\rho t[A^{-1}]^T[S][A^{-1}] \tag{43}$$

where:

$$S(i,j)=\frac{RL}{2}\left[\frac{\alpha_i\alpha_j+\beta_i\beta_j+1+\gamma_i\gamma_j+\delta_i\delta_j}{(\eta_i+\eta_j)}\right]\left[e^{(\eta_i+\eta_j)\varphi}-1\right] \quad if \quad \eta_i+\eta_j\neq 0$$
$$S(i,j)=\frac{RL\varphi}{2}\left(\alpha_i\alpha_j+\beta_i\beta_j+1+\gamma_i\gamma_j+\delta_i\delta_j\right) \quad if \quad \eta_i+\eta_j=0 \tag{44}$$

The stiffness matrix can be expressed as:

$$[k]=\int_0^L\int_0^{\varphi}[A^{-1}]^T\{[Q]^T[T]^T[P][T][Q]\}[A^{-1}]r\,dx\,d\theta \tag{45}$$

after integration, we obtain:

$$[k]=[A^{-1}]^T[G][A^{-1}] \tag{46}$$

The Gij's general element is defined as:

$$
\begin{aligned}
G(i,j)=\frac{RL}{2}[&P_{11}A_iA_j+P_{14}A_iD_j+P_{17}A_iG_j+P_{19}A_iI_j+\\
&P_{22}B_iB_j+P_{25}B_iE_j+P_{28}B_iH_j+P_{210}B_iJ_j+\\
&P_{33}C_iC_j+\\
&P_{41}D_iA_j+P_{44}D_iD_j+P_{47}D_iG_j+P_{49}D_iI_j+\\
&P_{52}E_iB_j+P_{55}E_iE_j+P_{58}E_iH_j+P_{510}E_iJ_j+\\
&P_{66}F_iF_j+\\
&P_{71}G_iA_j+P_{74}G_iD_j+P_{77}G_iG_j+P_{79}G_iI_j+\\
&P_{82}H_iB_j+P_{85}H_iE_j+P_{88}H_iH_j+P_{810}H_iJ_j+\\
&P_{91}I_iA_j+P_{94}I_iD_j+P_{97}I_iG_j+P_{99}I_iI_j+\\
&P_{102}J_iB_j+P_{105}J_iE_j+P_{108}J_iH_j+P_{1010}J_iJ_j]\\
&\times\left\{\frac{1}{(\eta_i+\eta_j)}\left(e^{(\eta_i+\eta_j)\varphi}-1\right)\right\} \qquad \text{if} \quad \eta_i+\eta_j\neq 0
\end{aligned}
\tag{47}
$$

$$
G(i,j)=\frac{RL\varphi}{2}[P_{11}A_iA_j+P_{14}A_iD_j+\cdots+P_{108}J_iH_j+P_{1010}J_iJ_j] \qquad \text{if} \quad \eta_i+\eta_j=0
$$

The [G] and [S] matrices were obtained analytically by carrying out the necessary matrix operations and integration over x and θ in equations (42) and (45). To do this it was found necessary to introduce several intermediate matrices, eventually obtaining expressions for the general terms k_{ij} and m_{ij} of [k] and [m], respectively. Because of the complexity of the manipulations, only the final results are given here. The A_i, B_i, C_i , ..., J_i components are given by [J] matrix.

6. <u>Stiffness and Mass Matrices for the Whole Shell in Vacuo -</u> As previously mentioned, the complete shell is divided into finite elements each of which is a cylindrical panel segment (Figure 6b). The global mass *[M]* and stiffness *[K]* matrices for the whole structure can be constructed whenever the mass *[m]* and stiffness matrices *[k]* for each element are obtained.

Each of these matrices (*[M]*& *[K]*) are of order *5(N+1)-J* where *N* is the total number of finite elements (Figure 6a) and *J* is the number of constraints applied.

The vectors $\{F_i\}$, $\{F_j\}$ represent the internal forces acting at nodes ***i*** and ***j***, respectively, and $\{\delta i\}$ are the corresponding displacements. As the shell is continuous, the sum of forces and moments at a particular node must be equal to external forces and moments applied at the node. Thus,

$$\{F\}^e = \{F_j\} + \{F_{i+1}\} \tag{48}$$

Morever, the displacement must be continuous, and

$$\{\delta_j\} = \{\delta_{i+1}\} \tag{49}$$

These relationships allow us to superimpose the mass and stiffness matrices of individual finite elements in order to obtain the global mass and stiffness matrices *[M]* and *[K]* for the whole shell in vacuo. The *[K]* and *[M]* matrices will be square matrices of order *5(N+1)*, where *N* is the number of finite elements.

7. ***Free Vibration -*** For free vibration, the equation of motion may be written in the form :

$$[M]\{\ddot{\Delta}\} + [K]\{\Delta\} = 0. \tag{50}$$

where $[\Delta] = \{\delta_1, \delta_2, \ldots, \delta_{N+1}\}T$, *N* is the number of finite elements, *[M]* and *[K]* are real, symmetric matrices of order $5(N+1) \times 5(N+1)$, and $\{\delta_{N+1}\}$ is the displacement vector associated with the lower edge of the last finite element. In the case where the shell has rigid edge constraints, the kinematic boundary conditions must be taken into account. Accordingly, *[K]* and *[M]* are reduced to square matrices of order *5(N+1)-J* , where *J* is the number of the constraint equations imposed. Thus,

$$\begin{Bmatrix} \delta_i \\ \delta_j \end{Bmatrix} = \left\{ U_i \;\; V_i \;\; W_i \;\; \beta_{x_i} \;\; \beta_{\theta_i} \;\; U_j \;\; V_j \;\; W_j \;\; \beta_{x_j} \;\; \beta_{\theta_j} \right\}^T = [A]_{(10\times10)} \; \{C\}_{(10\times1)} \tag{51}$$

Simply Supported : $v = w = \varphi_2 = N_1 = M_1 = 0$.

Clamped : $u = v = w = \varphi_1 = \varphi_2 = 0$.

Free : $N_1 = M_1 = Q_1 = N_6 = M_6 = 0$.

The solution of equation (50) now follows by standard matrix techniques, yielding the natural frequencies, ω_i, $i=1, 2, ..., 5(N+1)-J$ and the corresponding eigenvectors. It must be stressed that the mass and stiffness matrices obtained are associated with a specific axial wave number, ***m***, as is the nodal displacement vector. Thus the analysis is carried out independently for each ***m***.

8. ***Calculations and Discussion*** - As a numerical example, the non-dimensional fundamental frequencies of vibrations for simply-supported shell boundary conditions were computed for a four cross-ply layered (0°/90°/90°/0°) cylindrical shell. All layers are assumed to be of the same geometric and material parameters and the individual layer is assumed to be orthotropic. The following material properties are used:

$$E_1=25E_2 \; ; \; G_{23}=0.2E_2 \; ; \; G_{13}=G_{12}=0.5E_2 \; ; \; \nu_{12}=0.25 \; ; \; \rho=1$$

These results were compared with those of [Sciuva and Carrera 1992] to demonstrate the accuracy and range of applicability of the present theory. Also a comparison with CST (Hybrid finite element method based on classical shell theory) [Selmane and Lakis 1997] is given to illustrate the effect of transverse shear deformation. The results are shown in Table **I** for various length-to-radius ratios and for three radius-to-

thickness ratios.

The radius-to-thickness and the length-to-radius ratio effects are studied through this example. Comparison of the SDT (shear deformation theory) results with those of CST show that the shear deformation effect is significant for a length-to-radius ratio smaller than **1.0** for all ratios of R/t. For example, the solution reached by applying classical theory differs from that reached by SDT by 2% for L/R=50; 7% for L/R=1.0 and from 18% to up to 30% for L/R <= 0.1. All laminae which are used henceforth have the same properties as those of the first example.

In the following examples we study the effect of the axial mode (m) on the non-dimensional natural frequencies of cylindrical shells for different materials and geometry parameters. The graph showing different longitudinal vibration modes as a function of the circumferential wave number (n) are shown in figures 7-10. The first two show results for four symmetric layer cross-ply (0°/90°/90°/0°) laminated shells whose mechanical properties are the same as those of the shell in the previous example, but their radius-to-thickness ratios are different (R/t=50,100).

These graphs show reasonable agreement between the hybrid finite element method [Selmane and Lakis 1997] and the present theory for $m=1$ (about 4% difference). As can be seen, the influence of transverse shear deformation on the natural frequencies begins with increasing m. One may observe that the gap between the two theories increases as the axial mode (m) is increased and the radius-to-thickness ratio is decreased to a fixed value of L/R.

The mechanical parameters of the shell of the third example are listed in Table **II**. The interface is taken as the reference surface. It should be noted that, in this example, the laminate structure is composed of one lamina of steel and another of orthotropic material, so that all of the B_{ij} components (the extension-

bending, coupling, stiffness matrix) are not equal to zero, which means that the bending-stretching, coupling, and stiffness components are present. The results obtained are compared with those of classical shell theory.

The last example of this series (Figure 10) is made for isotropic material. In this graph, the natural frequencies are shown for longitudinal modes (m=1,3 and 5). It can be seen that, as expected, the frequencies are much closer for small values of m and n than for their large values.

The next two examples deal with the shear deformation effect on the natural frequencies of isotropic cylindrical shells for various values of the radius-to-thickness ratio. In the first (Figure 11), the non-dimensional natural frequencies are shown as a function of the circumferential wave number (n) for three different values of R/t and the fixed value of L/R and m. As can be seen, the transverse shear deformation causes the remarkable difference in the natural frequencies obtained from two theories for $R/t < 50$ and for values of n.

The variation of vibration parameter (Ω) of isotropic cylindrical shells with the radius-to-thickness ratio R/t is shown in (Figure 12) for two different values of axial mode number (m=2,3), fixed values of L/R, and circumferential wave number (n). This graph shows a greater difference between the results for $R/t \leq 25$ than for $R/t > 25$.

The variation of non-dimensional frequencies (Ω) as a function of the length-to-radius ratio L/R of isotropic and laminated anisotropic (having different symmetric 0°/90°/0°, 0°/90°/90°/0° and anti-symmetric 0°/90° lay-outs) are shown in (Figures 13-18). The effects of different values of R/t, L/t and axial mode numbers (m) are shown in these graphs.

In order to show clearly the difference between the results obtained from the two theories even for m=1, Figure (15) is replotted separately for m=1 (Figure 16) and m=5 (Figure 17). For the length-to-radius

ratio L/R <10 and high numbers of (m), there are always relatively large differences between the non-dimensional frequencies obtained from two different theories.

Figure (19) shows the non-dimensional fundamental natural frequencies (m=1) of cross-ply cylindrical shells for the symmetric lamination scheme (0°/90°/0°), for various different ratios of L/R, and for two values of L/t (L/t=10 & L/t=100).

Through these examples, a thickness study was carried out to determine the effect of transverse shear deformation. The thickness of the shell t was varied while L and R were kept constant. The geometries and material parameters as the same as in example *1* . The layers are of equal thickness.

The figures compare the results obtained from this theory with corresponding results given in references [Reddy 1984, Selmane and Lakis 1997, Sciuva and Carrera 1992]. The present results are always lower than the corresponding tabulated results of references [Reddy 1984, Reddy and Liu 1985, Sciuva and Carrera 1992]. However, some remarks should be made about these results.

As can be seen, the frequencies of symmetrically laminated shells for L/t=10 are less sensitive to R/L variations than those of thin shells L/t=100. Classical shell theory over-predicts, while the SDT under-estimates the frequencies even for very thin shells. Figures (20-23) show the non-dimensional frequencies of isotropic cylindrical shells vs. the thickness-to-radius ratio for three different radius-to-length ratios ($\lambda=m\pi R/L$) (m=1, n=1,2,3,4).

The results obtained from this work are shown along with those from other theories. There is good agreement between the results from this theory and those of reference [Bhimaraddi 1984]. In general, classical shell theory is seen to over-predict the natural frequencies when compared to the shear deformation theory. The error increases as values of n, R/L and t/R increase for a fixed value of **m**.

The two last examples involve the determination of the natural frequencies of an open cylindrical shell. Figure (24) shows the effect of variation of the length-to-radius ratio on the frequency parameters of an anisotropic (0°/90°/90°/0°) open cylindrical shell having both its straight and curved edges freely simply supported. Figure (25) is drawn for an isotropic open cylindrical shell having its straight edges clamped and the curved edges freely simply supported. The data are provided with the figures.

9. Conclusion - A particular method has been developed to determine the natural frequencies and the corresponding mode of vibrations for anisotropic, laminated and non-uniform, closed and open cylindrical shells by taking into account the shear deformation effect and rotary inertia as well as the initial curvature. The extensional and bending stiffness as well as the coupling of these two have been taken into account.

The method is a combination of hybrid finite element analysis and shear deformation theory of shells. It combines the advantage of finite element analysis and the precision of formulation which the use of displacement functions derived from shell theory contributes. The displacement functions for this theory are derived and the mass and stiffness matrices of each element are obtained by exact analytical integration.

Results of classical, hybrid finite element and shear deformation shell theories have been compared with the results of the present solution to emphasise the accuracy of this theory. Numerical results are presented for different materials (isotropic and cross-ply laminated materials having a symmetric and an anti-symmetric lay-up) and parametric studies including circumferential and axial wave number (n ; m); mean radius-to-thickness ratio (R/t); length-to-mean-radius ratio (L/R) and L/t; and the lamination scheme and number of layers are carried out through several numerical examples and results obtained are compared with

those of others, with good agreement, and with results obtained from the hybrid finite element method.

In general, classical shell theory over-estimates frequencies compared to the shear deformation theory especially for laminated anisotropic shells. It has been suggested that the reason for the difference is a change in shear angle from layer to layer and the insensitivity of the CST to this change.

The next step in this line of work will deal with liquid-filled open and closed non-uniform, anisotropic cylindrical shells by consideration of the shear deformation, rotary inertia and initial curvature effects.

Appendix

This appendix contains the equations of motion for the thin cylindrical anisotropic shell which is referred to in this work:

$$\gamma_{11}=h_1\frac{\partial u_1}{\partial y_1}+\frac{h_1u_2}{h_2}\frac{\partial h_1}{\partial y_2}+\frac{h_1u_3}{h_3}\frac{\partial h_1}{\partial y_3}$$

$$+\frac{1}{2}(\frac{\partial u_1}{\partial y_1}+\frac{u_2}{h_2}\frac{\partial h_1}{\partial y_2}+\frac{u_3}{h_3}\frac{\partial h_1}{\partial y_3})^2+\frac{1}{2}(\frac{\partial u_2}{\partial y_1}-\frac{u_1}{h_2}\frac{\partial h_1}{\partial y_2})^2+\frac{1}{2}(\frac{\partial u_3}{\partial y_1}-\frac{u_1}{h_3}\frac{\partial h_1}{\partial y_3})^2$$

$$\gamma_{22}=h_2\frac{\partial u_2}{\partial y_2}+\frac{h_2u_3}{h_3}\frac{\partial h_2}{\partial y_3}+\frac{h_2u_1}{h_1}\frac{\partial h_2}{\partial y_1}$$

$$+\frac{1}{2}(\frac{\partial u_2}{\partial y_2}+\frac{u_3}{h_3}\frac{\partial h_2}{\partial y_3}+\frac{u_1}{h_1}\frac{\partial h_2}{\partial y_1})^2+\frac{1}{2}(\frac{\partial u_3}{\partial y_2}-\frac{u_2}{h_3}\frac{\partial h_2}{\partial y_3})^2+\frac{1}{2}(\frac{\partial u_1}{\partial y_2}-\frac{u_2}{h_1}\frac{\partial h_2}{\partial y_1})^2$$

$$\gamma_{33}=h_3\frac{\partial u_3}{\partial y_3}+\frac{h_3u_1}{h_1}\frac{\partial h_3}{\partial y_1}+\frac{h_3u_2}{h_2}\frac{\partial h_3}{\partial y_2}$$

$$+\frac{1}{2}(\frac{\partial u_3}{\partial y_3}+\frac{u_1}{h_1}\frac{\partial h_3}{\partial y_1}+\frac{u_2}{h_2}\frac{\partial h_3}{\partial y_2})^2+\frac{1}{2}(\frac{\partial u_1}{\partial y_3}-\frac{u_3}{h_1}\frac{\partial h_3}{\partial y_1})^2+\frac{1}{2}(\frac{\partial u_2}{\partial y_3}-\frac{u_3}{h_2}\frac{\partial h_3}{\partial y_2})^2$$

$$\gamma_{12}=\frac{1}{2}(h_1\frac{\partial u_1}{\partial y_2}+h_2\frac{\partial u_2}{\partial y_1}-u_2\frac{\partial h_2}{\partial y_1}-u_1\frac{\partial h_1}{\partial y_2})$$

$$+\frac{1}{2}(\frac{\partial u_1}{\partial y_2}-\frac{u_2}{h_1}\partial h_2\partial y_1)(\frac{\partial u_1}{\partial y_1}+\frac{u_2}{h_2}\frac{\partial h_1}{\partial y_2}+\frac{u_3}{h_3}\frac{\partial h_1}{y_3})+\frac{1}{2}(\frac{\partial u_2}{\partial y_1}-\frac{u_1}{h_2}\frac{\partial h_1}{\partial y_2})(\frac{\partial u_2}{\partial y_2}+\frac{u_1}{h_1}\frac{\partial h_2}{\partial y_1}+\frac{u_3}{h_3}\frac{\partial h_2}{\partial y_3}) \qquad \text{(A-1)}$$

$$+\frac{1}{2}(\frac{\partial u_3}{\partial y_1}-\frac{u_1}{h_3}\frac{\partial h_1}{\partial y_3})(\frac{\partial u_3}{\partial y_2}-\frac{u_2}{h_3}\frac{\partial h_2}{\partial y_3})$$

$$\gamma_{13}=\frac{1}{2}(h_3\frac{\partial u_3}{\partial y_1}+h_1\frac{\partial u_1}{\partial y_3}-u_1\frac{\partial h_1}{\partial y_3}-u_3\frac{\partial h_3}{\partial y_1})$$

$$+\frac{1}{2}(\frac{\partial u_1}{\partial y_3}-\frac{u_3}{h_1}\frac{\partial h_3}{\partial y_1})(\frac{\partial u_1}{\partial y_1}+\frac{u_3}{h_3}\frac{\partial h_1}{\partial y_3}+\frac{u_2}{h_2}\frac{\partial h_1}{y_2})+\frac{1}{2}(\frac{\partial u_3}{\partial y_1}-\frac{u_1}{h_3}\frac{\partial h_1}{\partial y_3})(\frac{\partial u_3}{\partial y_3}+\frac{u_1}{h_1}\frac{\partial h_3}{\partial y_1}+\frac{u_2}{h_2}\frac{\partial h_3}{\partial y_2})$$

$$+\frac{1}{2}(\frac{\partial u_2}{\partial y_1}-\frac{u_1}{h_2}\frac{\partial h_1}{\partial y_2})(\frac{\partial u_2}{\partial y_3}-\frac{u_3}{h_2}\frac{\partial h_3}{\partial y_2})$$

$$\gamma_{23}=\frac{1}{2}(h_3\frac{\partial u_3}{\partial y_2}+h_2\frac{\partial u_2}{\partial y_3}-u_2\frac{\partial h_2}{\partial y_3}-u_3\frac{\partial h_3}{\partial y_2})$$

$$+\frac{1}{2}(\frac{\partial u_2}{\partial y_3}-\frac{u_3}{h_2}\frac{\partial h_3}{\partial y_2})(\frac{\partial u_2}{\partial y_2}+\frac{u_3}{h_3}\frac{\partial h_2}{\partial y_3}+\frac{u_1}{h_1}\frac{\partial h_2}{y_1})+\frac{1}{2}(\frac{\partial u_3}{\partial y_2}-\frac{u_2}{h_3}\frac{\partial h_2}{\partial y_3})(\frac{\partial u_3}{\partial y_3}+\frac{u_2}{h_2}\frac{\partial h_3}{\partial y_2}+\frac{u_1}{h_1}\frac{\partial h_3}{\partial y_1})$$

$$+\frac{1}{2}(\frac{\partial u_1}{\partial y_2}-\frac{u_2}{h_1}\frac{\partial h_2}{\partial y_1})(\frac{\partial u_1}{\partial y_3}-\frac{u_3}{h_1}\frac{\partial h_3}{\partial y_1})$$

The equation of motion for a cylindrical shell (equation 25):

$$
\begin{aligned}
&L_1(U,V,W,\beta_x,\beta_\theta,\overline{P_{ij}}) = \\
&P_{11}\frac{\partial^2 U_x}{\partial x^2}+\left(\frac{1}{R}(P_{15}+P_{51})-\frac{1}{2R^2}(P_{1,10}+P_{10,1})\right)\frac{\partial^2 U_x}{\partial x\partial\theta}+ \\
&+\left(\frac{P_{55}}{R^2}-\frac{(P_{10,5}+P_{5,10})}{2R^3}+\frac{P_{10,10}}{4R^4}\right)\frac{\partial^2 U_x}{\partial\theta^2}-I_1\frac{\partial^2 U_x}{\partial t^2}+ \\
&+(P_{12}+\frac{P_{18}}{2R})\frac{\partial^2 U_\theta}{\partial x^2}+\left(\frac{P_{58}}{2R^2}+\frac{1}{R}(P_{14}+P_{52})-\frac{P_{10,2}}{2R^2}-\frac{P_{10,8}}{4R^3}\right)\frac{\partial^2 U_\theta}{\partial x\partial\theta}+ \\
&+\left(\frac{P_{54}}{R^2}-\frac{P_{10,4}}{2R^3}\right)\frac{\partial^2 U_\theta}{\partial\theta^2}+\frac{P_{14}}{R}\frac{\partial W}{\partial x}+\left(\frac{P_{54}}{R^2}-\frac{P_{10,4}}{2R^3}\right)\frac{\partial W}{\partial\theta}+ \\
&P_{17}\frac{\partial^2\beta_x}{\partial x^2}+\left(\frac{1}{R}(P_{1,10}+P_{57})-\frac{P_{10,7}}{2R^2}\right)\frac{\partial^2\beta_x}{\partial x\partial\theta}+\left(\frac{P_{5,10}}{R^2}-\frac{P_{10,10}}{2R^3}\right)\frac{\partial^2\beta_x}{\partial\theta^2}-I_2\frac{\partial^2\beta_x}{\partial t^2}+ \\
&P_{18}\frac{\partial^2\beta_\theta}{\partial x^2}+\left(\frac{1}{R}(P_{19}+P_{58})-\frac{P_{10,8}}{2R^2}\right)\frac{\partial^2\beta_\theta}{\partial x\partial\theta}+\left(\frac{P_{5,9}}{R^2}-\frac{P_{10,9}}{2R^3}\right)\frac{\partial^2\beta_\theta}{\partial\theta^2}
\end{aligned}
$$

$$
\begin{aligned}
&L_2(U,V,W,\beta_x,\beta_\theta,\overline{P_{ij}}) = \\
&\left(\frac{P_{81}}{2R}+P_{21}\right)\frac{\partial^2 U_x}{\partial x^2}+\left(\frac{1}{R}(P_{25}+P_{41})+\frac{P_{85}}{2R^2}-\frac{P_{8,10}}{4R^3}-\frac{P_{2,10}}{2R^2}\right)\frac{\partial^2 U_x}{\partial x\partial\theta}+ \\
&+\left(\frac{P_{45}}{R^2}-\frac{P_{4,10}}{2R^3}\right)\frac{\partial^2 U_x}{\partial\theta^2}+ \\
&\left(\frac{P_{82}}{2R}+\frac{P_{88}}{4R^2}+P_{22}+\frac{P_{28}}{R}\right)\frac{\partial^2 U_\theta}{\partial x^2}+\left(\frac{1}{R}(P_{24}+P_{42})+\frac{1}{2R^2}(P_{48}+P_{84})\right)\frac{\partial^2 U_\theta}{\partial x\partial\theta}+ \\
&+\frac{P_{44}}{R^2}\frac{\partial^2 U_\theta}{\partial\theta^2}-\frac{P_{66}}{R^2}U_\theta-I_1\frac{\partial^2 U_\theta}{\partial t^2}+ \\
&+\left(\frac{1}{R}(P_{24}+P_{63})+\frac{P_{84}}{2R^2}\right)\frac{\partial W}{\partial x}+\frac{1}{R^2}(P_{44}+P_{66})\frac{\partial W}{\partial\theta}+ \\
&+\left(\frac{P_{87}}{2R}+P_{27}\right)\frac{\partial^2\beta_x}{\partial x^2}+\left(\frac{1}{R}(P_{2,10}+P_{47})+\frac{P_{8,10}}{2R^2}\right)\frac{\partial^2\beta_x}{\partial x\partial\theta}+ \\
&+\frac{P_{4,10}}{R^2}\frac{\partial^2\beta_x}{\partial\theta^2}+\frac{P_{63}}{R}\beta_x+ \\
&+\left(\frac{P_{88}}{2R}+P_{28}\right)\frac{\partial^2\beta_\theta}{\partial x^2}+\left(\frac{1}{R}(P_{29}+P_{48})+\frac{P_{89}}{2R^2}\right)\frac{\partial^2\beta_\theta}{\partial x\partial\theta}+ \\
&+\frac{P_{49}}{R^2}\frac{\partial^2\beta_\theta}{\partial\theta^2}+\frac{P_{66}}{R}\beta_\theta-I_2\frac{\partial^2\beta_\theta}{\partial t^2}
\end{aligned}
\qquad \text{(A-2,3,4)}
$$

$$
\begin{aligned}
&L_3(U,V,W,\beta_x,\beta_\theta,\overline{P_{ij}}) = \\
&-\frac{P_{41}}{R}\frac{\partial U_x}{\partial x}+\left(\frac{P_{4,10}}{2R^3}-\frac{P_{45}}{R^2}\right)\frac{\partial U_x}{\partial\theta}- \\
&-\frac{1}{R}\left(P_{36}+P_{42}+\frac{P_{48}}{2R}\right)\frac{\partial U_\theta}{\partial x}-\frac{1}{R^2}(P_{44}+P_{66})\frac{\partial U_\theta}{\partial\theta}+ \\
&+P_{33}\frac{\partial^2 W}{\partial x^2}+\frac{1}{R}(P_{63}+P_{36})\frac{\partial^2 W}{\partial x\partial\theta}+\frac{P_{66}}{R^2}\frac{\partial^2 W}{\partial\theta^2}-\frac{P_{44}}{R^2}W-I_1\frac{\partial^2 W}{\partial t^2}+ \\
&+\left(P_{33}-\frac{P_{47}}{R}\right)\frac{\partial\beta_x}{\partial x}+\frac{1}{R}\left(P_{63}-\frac{P_{4,10}}{R}\right)\frac{\partial\beta_x}{\partial\theta}+ \\
&+\left(P_{36}-\frac{P_{48}}{R}\right)\frac{\partial\beta_\theta}{\partial x}+\frac{1}{R}\left(P_{66}-\frac{P_{49}}{R}\right)\frac{\partial\beta_\theta}{\partial\theta}
\end{aligned}
$$

$$L_4(U,V,W,\beta_x,\beta_\theta,\overline{P_{ij}}) =$$
$$P_{71}\frac{\partial^2}{\partial x^2}+(\frac{1}{R}(P_{75}+P_{10,1})-\frac{P_{7,10}}{2R^2})\frac{\partial^2}{\partial x\partial\theta}+(\frac{P_{10,5}}{R^2}-\frac{P_{10,10}}{2R^3})\frac{\partial^2 U_x}{\partial\theta^2}-I_2\frac{\partial^2 U_x}{\partial t^2}+$$
$$+(P_{72}+\frac{P_{78}}{2R})\frac{\partial^2 U_\theta}{\partial x^2}+(\frac{1}{R}(P_{74}+P_{10,2})+\frac{P_{10,8}}{2R^2})\frac{\partial^2 U_\theta}{\partial x\partial\theta}+\frac{P_{10,4}}{R^2}\frac{\partial^2 U_\theta}{\partial\theta^2}+\frac{P_{36}}{R}U_\theta+$$
$$+(\frac{P_{74}}{R}-P_{33})\frac{\partial W}{\partial x}+\frac{1}{R}(\frac{P_{10,4}}{R}-P_{36})\frac{\partial W}{\partial\theta}+$$
$$+P_{77}\frac{\partial^2\beta_x}{\partial x^2}+\frac{1}{R}(P_{7,10}+P_{10,7})\frac{\partial^2\beta_x}{\partial x\partial\theta}+\frac{P_{10,10}}{R^2}\frac{\partial^2\beta_x}{\partial\theta^2}-P_{33}\beta x-I_3\frac{\partial^2\beta_x}{\partial t^2}+$$
$$P_{78}\frac{\partial^2\beta_\theta}{\partial x^2}+\frac{1}{R}(P_{79}+P_{10,8})\frac{\partial^2\beta_\theta}{\partial x\partial\theta}+\frac{P_{10,9}}{R^2}\frac{\partial^2\beta_\theta}{\partial\theta^2}-P_{36}\beta_\theta$$

$$L_5(U,V,W,\beta_x,\beta_\theta,\overline{P_{ij}}) =$$
$$P_{81}\frac{\partial U_x^2}{\partial x^2}+(\frac{1}{R}(P_{85}+P_{91})-\frac{P_{8,10}}{2R^2})\frac{\partial^2 U_x}{\partial x\partial\theta}+(\frac{P_{95}}{R^2}-\frac{P_{9,10}}{2R^3})\frac{\partial^2 U_x}{\partial\theta^2}+$$
$$(P_{82}+\frac{P_{88}}{2R})\frac{\partial^2 U_\theta}{\partial x^2}+(\frac{1}{R}(P_{84}+P_{92})+\frac{P_{98}}{2R^2})\frac{\partial^2 U_\theta}{\partial x\partial\theta}+$$
$$+\frac{P_{94}}{R^2}\frac{\partial^2 U_\theta}{\partial\theta^2}+\frac{P_{66}}{R}U_\theta-I_2\frac{\partial^2 U_\theta}{\partial t^2}+$$
$$+(\frac{P_{84}}{R}-P_{63})\frac{\partial W}{\partial x}+\frac{1}{R}(\frac{P_{94}}{R}-P_{66})\frac{\partial W}{\partial\theta}+$$
$$P_{87}\frac{\partial^2\beta_x}{\partial x^2}+\frac{1}{R}(P_{97}+P_{8,10})\frac{\partial^2\beta_x}{\partial x\partial\theta}+\frac{P_{9,10}}{R^2}\frac{\partial^2\beta_x}{\partial\theta^2}-P_{63}\beta_x+$$
$$P_{88}\frac{\partial^2\beta_\theta}{\partial x^2}+\frac{1}{R}(P_{89}+P_{98})\frac{\partial^2\beta_\theta}{\partial x\partial\theta}+\frac{P_{99}}{R^2}\frac{\partial^2\beta_\theta}{\partial\theta^2}-P_{66}\beta_\theta-I_3\frac{\partial^2\beta_\theta}{\partial t^2}$$

(A-5,6)

$$\begin{Bmatrix} N_{xx} \\ N_{x\theta} \\ Q_{xx} \\ N_{\theta\theta} \\ N_{\theta x} \\ Q_{\theta\theta} \\ M_{xx} \\ M_{x\theta} \\ M_{\theta\theta} \\ M_{\theta x} \end{Bmatrix} = \begin{bmatrix} A_{11}+\frac{B_{11}}{R} & 2(A_{16}+\frac{B_{16}}{R}) & 0 & A_{12}+\frac{B_{12}}{R} & 2(A_{16}+\frac{B_{16}}{R}) & 0 & B_{11}+\frac{D_{11}}{R} & 2(B_{16}+\frac{D_{16}}{R}) & B_{12}+\frac{D_{12}}{R} & 2(B_{16}+\frac{D_{16}}{R}) \\ A_{61}+\frac{B_{61}}{R} & 2(A_{66}+\frac{B_{66}}{R}) & 0 & A_{62}+\frac{B_{62}}{R} & 2(A_{66}+\frac{B_{66}}{R}) & 0 & B_{61}+\frac{D_{61}}{R} & 2(B_{66}+\frac{D_{66}}{R}) & B_{62}+\frac{D_{62}}{R} & 2(B_{66}+\frac{D_{66}}{R}) \\ 0 & 0 & 2(A_{55}+\frac{B_{55}}{R}) & 0 & 0 & 2(A_{45}+\frac{B_{45}}{R}) & 0 & 0 & 0 & 0 \\ A_{21} & 2A_{26} & 0 & A_{22} & 2A_{26} & 0 & B_{21} & 2B_{26} & B_{22} & 2B_{26} \\ A_{61} & 2A_{66} & 0 & A_{62} & 2A_{66} & 0 & B_{61} & 2B_{66} & B_{62} & 2B_{66} \\ 0 & 0 & 2A_{45} & 0 & 0 & 2A_{44} & 0 & 0 & 0 & 0 \\ B_{11}+\frac{D_{11}}{R} & 2(B_{16}+\frac{D_{16}}{R}) & 0 & B_{12}+\frac{D_{12}}{R} & 2(B_{16}+\frac{D_{16}}{R}) & 0 & D_{11}+\frac{E_{11}}{R} & 2(D_{16}+\frac{E_{16}}{R}) & D_{12}+\frac{E_{12}}{R} & 2(D_{16}+\frac{E_{16}}{R}) \\ B_{61}+\frac{D_{61}}{R} & 2(B_{66}+\frac{D_{66}}{R}) & 0 & B_{62}+\frac{D_{62}}{R} & 2(B_{66}+\frac{D_{66}}{R}) & 0 & D_{61}+\frac{E_{61}}{R} & 2(D_{66}+\frac{E_{66}}{R}) & D_{62}+\frac{E_{62}}{R} & 2(D_{66}+\frac{E_{66}}{R}) \\ B_{21} & 2B_{26} & 0 & B_{22} & 2B_{26} & 0 & D_{21} & 2D_{26} & D_{22} & 2D_{26} \\ B_{61} & 2B_{66} & 0 & B_{62} & 2B_{66} & 0 & D_{61} & 2D_{66} & D_{62} & 2D_{66} \end{bmatrix}_{(10\times10)} \begin{Bmatrix} \varepsilon^o_x \\ \gamma^o_x \\ \mu^o_x \\ \varepsilon^o_\theta \\ \gamma^o_\theta \\ \mu^o_\theta \\ \kappa_x \\ \tau_x \\ \kappa_\theta \\ \tau_\theta \end{Bmatrix}_{(10\times1)} \quad \text{(A-7)}$$

Matrix [H]:

$$\begin{bmatrix} H_{11} & H_{12} & H_{13} & H_{14} & H_{15} \\ H_{21} & H_{22} & H_{23} & H_{24} & H_{25} \\ H_{31} & H_{32} & H_{33} & H_{34} & H_{35} \\ H_{41} & H_{42} & H_{43} & H_{44} & H_{45} \\ H_{51} & H_{52} & H_{53} & H_{54} & H_{55} \end{bmatrix} \begin{Bmatrix} A \\ B \\ C \\ D \\ E \end{Bmatrix} = \begin{Bmatrix} 0 \\ 0 \\ 0 \\ 0 \\ 0 \end{Bmatrix}$$

where:

$$H_{11}=P_{11}(-\bar{m}^2)-[\frac{P_{5,10}+P_{10,5}}{2R^3}-\frac{P_{10,10}}{4R^4}-\frac{P_{55}}{R^2}]\eta^2-[\frac{P_{15}+P_{51}}{R}-\frac{P_{10,1}+P_{1,10}}{2R^2}](\bar{m}\eta)$$

$$H_{12}=(P_{12}+\frac{P_{18}}{2R})(-\bar{m}^2)+[\frac{P_{14}+P_{52}}{R}+\frac{P_{58}-P_{10,2}}{2R^2}-\frac{P_{10,8}}{4R^3}]\bar{m}\eta+(\frac{P_{54}}{R^2}-\frac{P_{10,4}}{2R^3})\eta^2$$

$$H_{13}=\frac{P_{14}}{R}\bar{m}+(\frac{P_{54}}{R^2}-\frac{P_{10,4}}{2R^3})\eta$$

$$H_{14}=P_{17}(-\bar{m}^2)-[\frac{P_{1,10}+P_{57}}{R}-\frac{P_{10,7}}{2R^2}]\bar{m}\eta-(\frac{P_{10,10}}{2R^3}-\frac{P_{5,10}}{R^2})\eta^2$$

$$H_{15}=P_{18}(-\bar{m}^2)+[\frac{P_{19}+P_{58}}{R}-\frac{P_{10,8}}{2R^2}]\bar{m}\eta-(\frac{P_{10,9}}{2R^3}-\frac{P_{59}}{R^2})\eta^2$$

$$H_{22}=[P_{22}+\frac{P_{28}+P_{82}}{2R}+\frac{P_{88}}{4R^2}](-\bar{m}^2)+[\frac{P_{24}+P_{42}}{R}+\frac{P_{48}+P_{84}}{2R^2}]\bar{m}\eta-\frac{1}{R^2}(P_{66}-P_{44}\eta^2)$$

$$H_{23}=(\frac{P_{24}+P_{63}}{R}+\frac{P_{84}}{2R^2})\bar{m}+(P_{44}+P_{66})\frac{\eta}{R^2} \qquad \text{(A-8)}$$

$$H_{24}=(P_{27}+\frac{P_{87}}{2R})(-\bar{m}^2)-[\frac{P_{2,10}+P_{47}}{R}+\frac{P_{8,10}}{2R^2}]\bar{m}\eta+\frac{\eta^2}{R^2}P_{4,10}+\frac{P_{63}}{R}$$

$$H_{25}=(P_{28}+\frac{P_{88}}{2R})(-\bar{m}^2)+(\frac{P_{29}+P_{48}}{R}+\frac{P_{89}}{2R^2})\bar{m}\eta+\frac{P_{49}}{R^2}\eta^2+\frac{P_{66}}{R}$$

$$H_{33}=P_{33}(-\bar{m}^2)+(\frac{P_{36}+P_{63}}{R})\bar{m}\eta+\frac{P_{66}}{R^2}\eta^2-\frac{P_{44}}{R^2}$$

$$H_{34}=(\frac{P_{47}}{R}-P_{33})(\bar{m})+(\frac{P_{63}}{R}-\frac{P_{4,10}}{R^2})\eta$$

$$H_{35}=(P_{36}-\frac{P_{48}}{R})(\bar{m})+(P_{66}-\frac{P_{49}}{R})\frac{\eta}{R}$$

$$H_{44}=P_{77}(-\bar{m}^2)-(P_{7,10}+P_{10,7})\frac{\bar{m}\eta}{R}+\frac{P_{10,10}}{R^2}\eta^2-P_{33}$$

$$H_{45}=P_{78}(-\bar{m}^2)+(P_{79}+P_{10,8})\frac{\bar{m}\eta}{R}+P_{10,9}\frac{\eta^2}{R^2}-P_{36}$$

$$H_{55}=P_{88}(-\bar{m}^2)+(P_{98}+P_{89})\frac{\bar{m}\eta}{R}+\frac{P_{99}}{R^2}\eta^2-P_{66}$$

where

$$\bar{m}=\frac{m\pi}{L}$$

Matrix [LL]:

$$
\begin{aligned}
&LL(1,j)=\alpha_j \\
&LL(2,j)=\beta_j \\
&LL(3,j)=1 \qquad\qquad j=1,2,..,10 \\
&LL(4,j)=\gamma_j \\
&LL(5,j)=\delta_j \\
&X(i,j)=e^{\eta_i\theta} \quad if \quad i=j \\
&\qquad\qquad i,j=1,2,...,10 \\
&X(i,j)=0. \quad if \quad i\neq j
\end{aligned}
\tag{A-9}
$$

Matrix [A]:

$$
\begin{aligned}
&A(1,j)=\alpha_j \;;\; A(6,j)=A(1,j)a_j \\
&A(2,j)=\beta_j \;;\; A(7,j)=A(2,j)a_j \\
&A(3,j)=1 \;;\; A(8,j)=a_j \qquad a_j=e^{\eta_j\varphi} \quad j=1,2,...,10 \\
&A(4,j)=\gamma_j \;;\; A(9,j)=A(4,j)a_j \\
&A(5,j)=\delta_j \;;\; A(10,j)=A(5,j)a_j
\end{aligned}
\tag{A-10}
$$

Matrices [QQ] and [J] :

$$
\{\varepsilon\}=[T]_{(10\times10)}[QQ]_{(10\times10)}[A]^{-1}_{(10\times10)}\begin{Bmatrix}\delta_i\\ \delta_j\end{Bmatrix}_{(10\times1)}
\tag{A-11}
$$

$$
With:\ [QQ]_{(10\times10)}=[J]_{(10\times10)}[X]_{(10\times10)}
$$

$$
\begin{aligned}
&J(1,j)=-\alpha_j\bar{m} \;;\; J(6,j)=\frac{1}{R}(\eta_j-\beta_j)+\delta_j \\
&J(2,j)=\beta_j\bar{m} \;;\; J(7,j)=-\gamma_j\bar{m} \\
&J(3,j)=\gamma_j+\bar{m} \;;\; J(8,j)=\delta_j\bar{m}+\frac{\bar{m}}{2R}\beta_j \qquad j=1,...,10 \\
&J(4,j)=\frac{1}{R}(1+\eta_j\beta_j) \;;\; J(9,j)=\frac{1}{R}\eta_j\delta_j \\
&J(5,j)=\frac{1}{R}(\eta_j\alpha_j) \;;\; J(10,j)=\frac{1}{R}\eta_j\gamma_j-\frac{1}{2R^2}\eta_j\alpha_j \\
&\qquad where: \\
&\qquad \bar{m}=\frac{m\pi}{L}
\end{aligned}
\tag{A-12}
$$

REFERENCES

[1] Ambartsumyan, S.A. Theory of Anisotropic Shells. NASA-TT-F-118, 1964.

[2] Bert, C.W. Analysis of Shells. In:Broutman LJ, editor. Analysis and Performance of Composites. New York: John Wiley, 1980: 207-258.

[3] Bhimaraddi, A. A Higher Order Theory for Free Vibration Analysis of Circular Cylindrical Shells. Int. J. Solids Struc. 1984; **20 (7)**: 623-630.

[4] Dong, S.B., Pister, K.S., Taylor, R.L. On the Theory of Laminated Anisotropic Shells and Plates. Journal of Aero. Sci. 1962; **29**: 969-975.

[5] Dong, S.B., Tso, F.K.W. On a Laminated Orthotropic Shell Theory Including Transverse Shear Deformation. J. Applied Mechanics 1972; **39**: 1091-1096.

[6] Grigolyuk, E.I., Kulikov, G.M. General Direction of Development of the Theory of Multi-layered Shells. Mechanics of Composite Materials 1988; **24(2)**: PP 231-241.

[7] Gulati, S.T., Essenberg, F. Effects of Anisotropy in Axisymmetric Cylindrical Shells. Journal of Applied Mechanics 1967; **34**: 650-666.

[8] Hilderbrand, F.B., Reissner, E., Thomas, G.B. Notes on the Foundations of the Theory of Small Displacements of Orthotropic Shells. NACA-TN-1833, 1949.

[9] Hsu, T.M., Wang, J.T.S. A Theory of Laminated Cylindrical Shells Consisting of Layers of Orthotropic Laminae. AIAA Journal 1970; **8(12)**: 2141-2146.

[10] Jing, H.S., Tzeng, K.G. Approximate Elasticity Solution for Laminated Anisotropic Finite Cylinders. AIAA Journal 1993; **31(11)**: 2121-2129.

[11] Koiter, W.T. A Consistent First Approximation in the General Theory of Thin Elastic Shells. Pro. Sym. on Theory of Thin Elastic Shells, Amsterdam, North Holland 1960: 12-32.

[12] Kraus, H. Thin Elastic Shells. New York: John Wiley, 1967.

[13] Lakis, A.A., Païdoussis, M.P. Free Vibration of Cylindrical Shells Partially Filled with Liquid. Journal of Sound and Vibration 1971; **19**: 1-15.

[14] Lakis, A.A., Païdoussis, M.P. Prediction of the Response of a Cylindrical Shell to Arbitrary of Boundary Layer-Induced Random Pressure Field. Journal of Sound and Vibration 1972; **25**:1-27. [15] Lakis, A.A., Païdoussis, M.P. Dynamic Analysis of Axially Non-Uniform Thin Cylindrical Shells. Journal of Mech. Eng. Science 1972; **14(1)**: 49-71.

[16] Lakis, A.A. Effects of Fluid Pressures on the Vibration Characteristics of Cylindrical Vessels. Proc. of the Int. Conf. on Pressure Surges, London, UK 1976: 11-15.

[17] Lakis, A.A., Doré, R. General Method for Analysing Contact Stresses on Cylindrical Vessels. Int. J. Solids and Struct. 1978; **14(6)**: 499-516.

[18] Lakis, A.A., Tuy, N.Q., Selmane, A. Analysis of Axially Non-Uniform Thin Spherical Shells. Proc. of the Int. Symposium on Structural Analysis and Optimization, Paris, France 1989: 80-85. [19] Lakis, A.A., Laveau, A. Non-Linear Dynamic of Anisotropic Cylindrical Shells Containing A Flowing Fluid. Int. J. Solids and Struct. 1991; **28(9)**: 1079-1094.

[20] Lakis, A.A., Sinno, M. Free Vibration of Axisymmetric and Beam-Like Cylindrical Shells Partially Filled with Liquid. Int. J. For Num. Meth. in Eng. 1992; **33**: 235-268.

[21] Lakis, A.A., Van Dyke, P., Ouriche, H. Dynamic Analysis of Anisotropic Fluid-Filled Conical Shells. Journal of Fluids and Struct. 1992; **6**: 135-162.

[22] Leissa, A.W. Vibration of Shells. NASA SP-288, 1973.

[23] Leissa, A.W, Lee JK, Wang AJ. Vibrations of Cantilevered Shallow Cylindrical Shells of Rectangular Platform. Journal of Sound and Vibration 1981; **78(3)**: 311-328.

[24] Naghdi, P.M. A Survey of Recent Progress in the Theory of Elastic Shells. Applied Mechanics Reviews 1956; **9(9)**: 365-388.

[25] Naghdi, P.M. On the Theory of Thin Elastic Shells. Quart. Appl. Math.1957; **14**: 369-380.

[26] Noor, A.K., Peters JM. Vibration analysis of Laminated anisotropic Shells of Revolution. Computer Meth. in Appl. Mech. and Eng. 1987; **61**: 277-301.

[27] Novozhilov, V.V. The Theory of Thin Shells P. Noordhoff Ltd., 1959.

[28] Reddy, J.N. Exact Solutions of Moderately Thick Laminated Shells. Journal of Eng. Mech., ASCE 1984; **110 (5)**: 794-809.

[29] Reddy, J.N., Liu, C.F. A Higher Order Shear Deformation Theory of Laminated Elastic Shells. Int. J. Engng. Sci. 1985; **23(3)**: 319-330.

[30] Reissner, E. On a Variational Theorem in Elasticity. Journal Math. and Physics 1950; **29**: 90-95.

[31] Reissner, E. Stress-strain Relation in The Theory of Thin Elastic Shells. Journal Math. Phys. 1952; **31**: 109-119.

[32] Ren, J.G. Analysis of Simply Supported Laminated Circular Cylindrical Shell Roofs. Composite Science and Technology 1989; **11(4)**: 277-292.

[33] Saada, A.S. Elasticity Theory and Applications. Pergamon Press, 1993.

[34] Sanders, J.L. An Improved First Approximation Theory for Thin Shells. NASA 1959, **TRR-24**:1-23.

[35] Sanders, J.L. Nonlinear Theories for Thin Shells. Appl. Math.1962; **XXI(1)**: 21-36.

[36] Sciuva, M.D., Carrera, E. Elastodynamic Behavior of Relatively Thick, Symmetrically Laminated, Anisotropic Circular Cylindrical Shells. Transaction of the ASME 1992; **59**: 222-224. [37] Selmane, A., Lakis, A.A. Vibration Analysis of Anisotropic Open Cylindrical Shells Containing Flowing Fluid. Journal of Fluids and Structures 1997; **11**: 111-134.

[38] Selmane, A., Lakis, A.A. Influence of Geometric Non-Linearities on the Vibration of Orthotropic Open Cylindrical Shells. Int. Journal for Numerical Methods in Engineering 1997; **40**:1115-1137.

[39] Selmane, A., Lakis, A.A. Non-Linear Dynamic Analysis of Orthotropic Open Cylindrical Shells Subjected to a Flowing Fluid. Journal of Sound and Vibration 1997; **202(1)**: 67-93.

[40] Selmane, A., Lakis, A.A. Dynamic Analysis of Anisotropic Open Cylindrical Shells. Journal of Computer and Structures 1997; **62(1)**: 1-12.

[41] Toorani, M.H., Lakis, A.A. Effects of Transverse Shear Deformations and Rotary Inertia on the General Equations of Anisotropic Plates and Shells. Tech. Report, No. EPM/RT-99/3, 1999, École Polytechnique de Montréal, Canada.

[42] Voyiadjis, G.Z., Shi, G. A Refined Two-Dimensional Theory for Thick Cylindrical Shells. Int. Journal of Solids and Struct. 1991; **27(3)**: 261-282.

Table I

Non-dimensional fundamental frequencies (m=1) of simply-supported cylindrical shells with symmetric cross-ply 0°/90°/90°/0° $\Omega = \omega_0 R^2 \sqrt{\rho/E_2}\,/\,t$

	R/t=100				R/t=50				R/t=20			
L/R	**CST[1]**	**HFE[2]**	**SDT[3]**	**PRE[4]**	**CST[1]**	**HFE[2]**	**SDT[3]**	**PRE[4]**	**CST[1]**	**HFE[2]**	**SDT[3]**	**PRE[4]**
0.10	1409	1421	1160	1154	1120	1200	815.5	764.9	448.3	520.4	384.3	354.5
0.25	248	259.3	240.7	235.6	233.1	265.7	205.4	205.4	220.0	230.4	132.5	122.8
0.5	83.45	86.49	82.96	82.47	70.07	72.53	68.04	65.12	59.24	61.88	50.02	47.53
1	38.72	39.03	38.69	35.87	27.31	27.59	27.18	25.33	18.82	19.70	18.15	17.52
2.5	17.52	17.54	17.51	16.16	11.49	11.50	11.48	10.73	6.55	6.54	6.53	6.20
5	9.37	9.376	9.37	9.053	6.28	6.28	6.28	5.92	3.70	3.70	3.70	3.31
10	4.76	4.760	4.76	4.761	3.53	3.52	3.53	3.50	1.73	1.73	1.73	1.68
25	1.74	1.736	1.74	1.704	1.27	1.27	1.27	1.12	.74	.74	.74	.7347
50	1.08	1.080	1.08	1.0296	.54	.54	.54	.53	.22	.22	.22	.2151

1)CST : Classical shell theory [36]

2)HFE : Hybrid finite element method [40], these results were obtained by authors

3)SDT : Shear deformation theory[36]

4)Present Theory : (Hybrid finite element method + Shear Deformation , Rotary Inertia and Initial Curvature Effects)

Table II

Properties of the shell layers

Layer	Q_{11}(psi)	Q_{12}(psi)	Q_{22}(psi)	Q_{66}(psi)	Thickness (inches)	Density
1	6.70×10^6	2.11×10^6	12.00×10^6	2.51×10^6	0.20	0.5ρ
2	33.00×10^6	11.00×10^6	33.00×10^6	13.20×10^6	0.20	1.0ρ

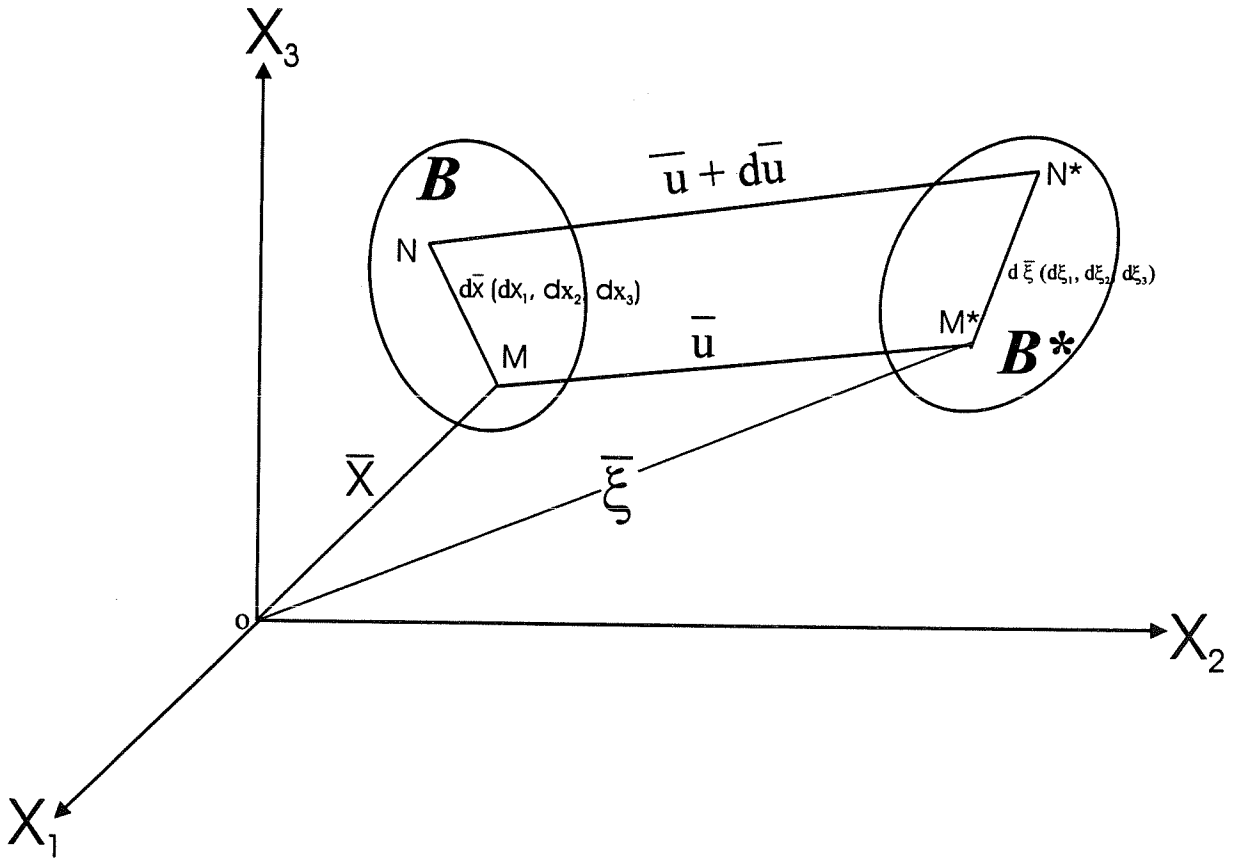

Figure 1: Segment MN deforms to M*N* through displacement vector

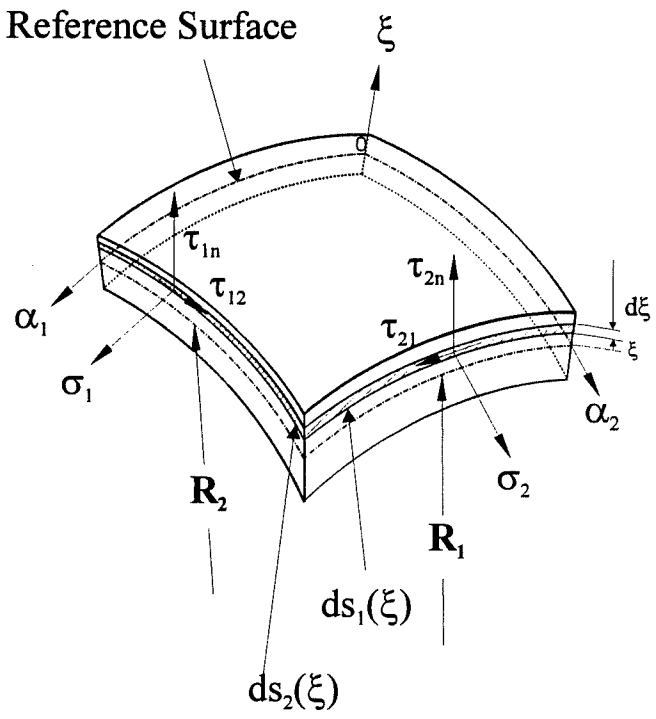

Figure 2: Surface and shell coordinate system.

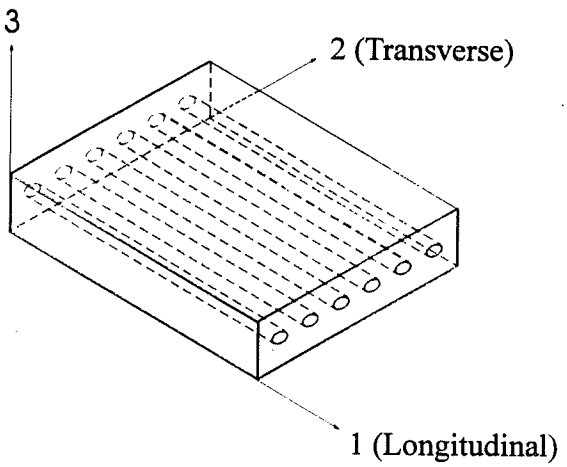

Figure 3: Unidirectional lamina and principal coordinate axes.

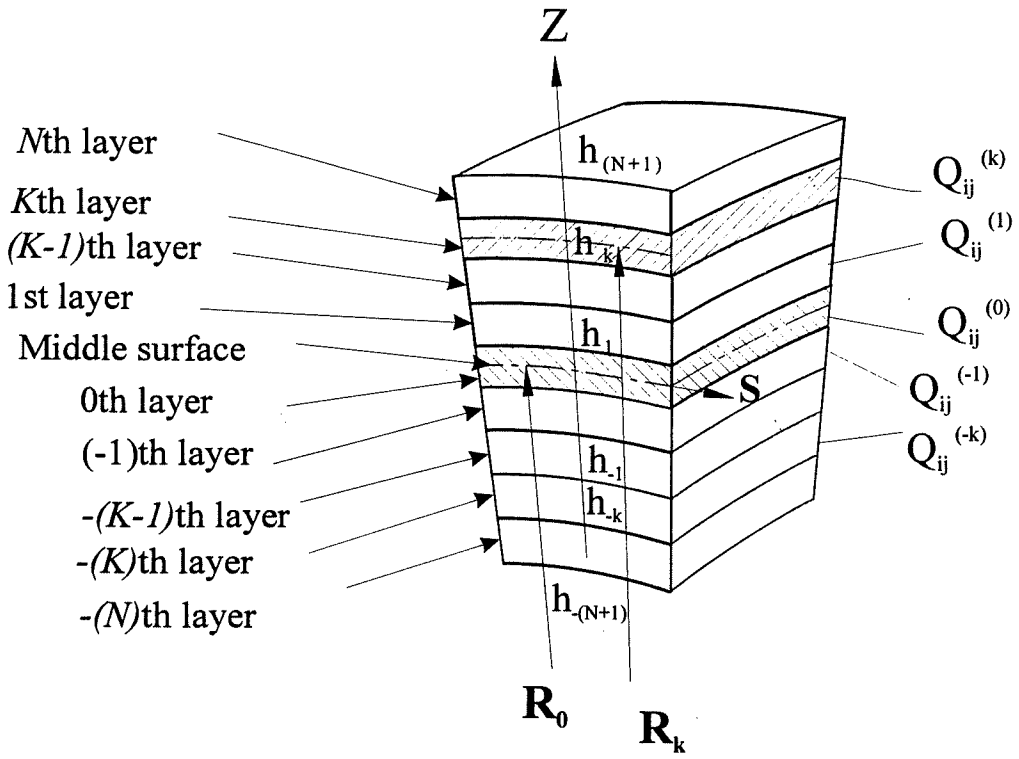

(A)

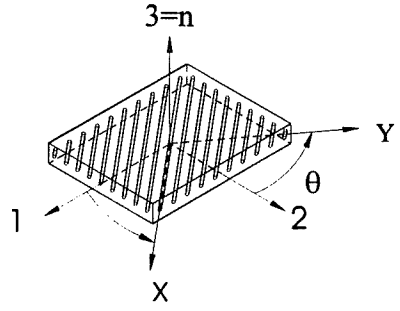

(B)

Figure 4: a)Multidirectional laminate with coordinate notation of individual plies.
b)A fibre reinforced lamina with global and material coordinate systems.

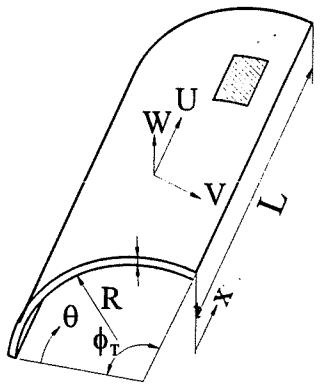

(A)

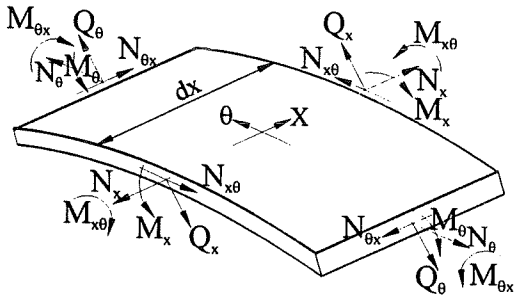

(B)

Figure 5: a)Circular cylindrical shell geometry.
b)Positive directions of integrated stress quantities.

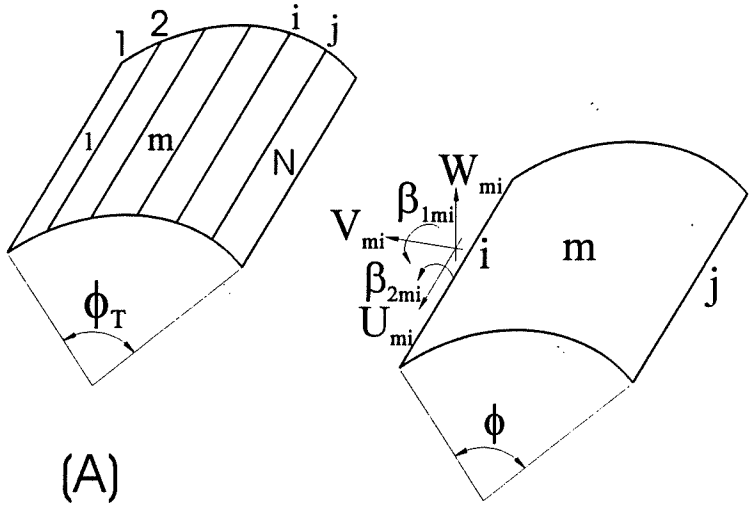

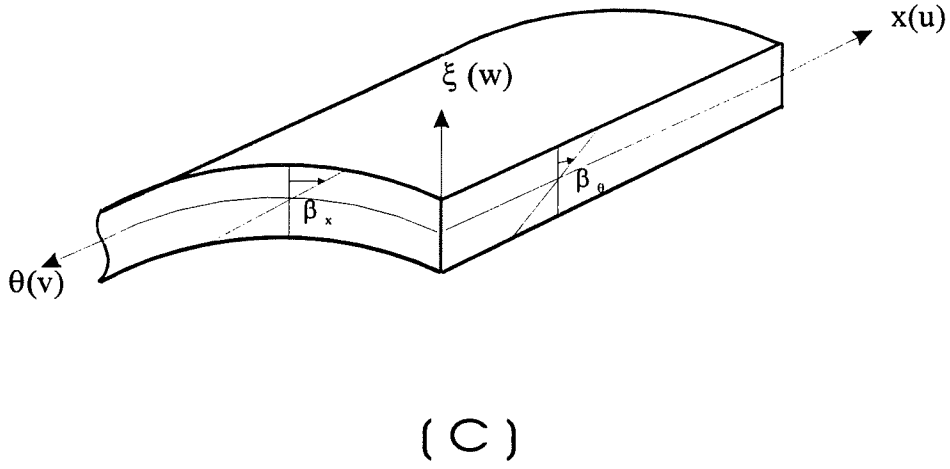

Figure 6: a)Finite element discretization.
b)Nodal displacement at node ***i*** for the ***m***'th element. N: Number of elements.
c) Definition of variables.

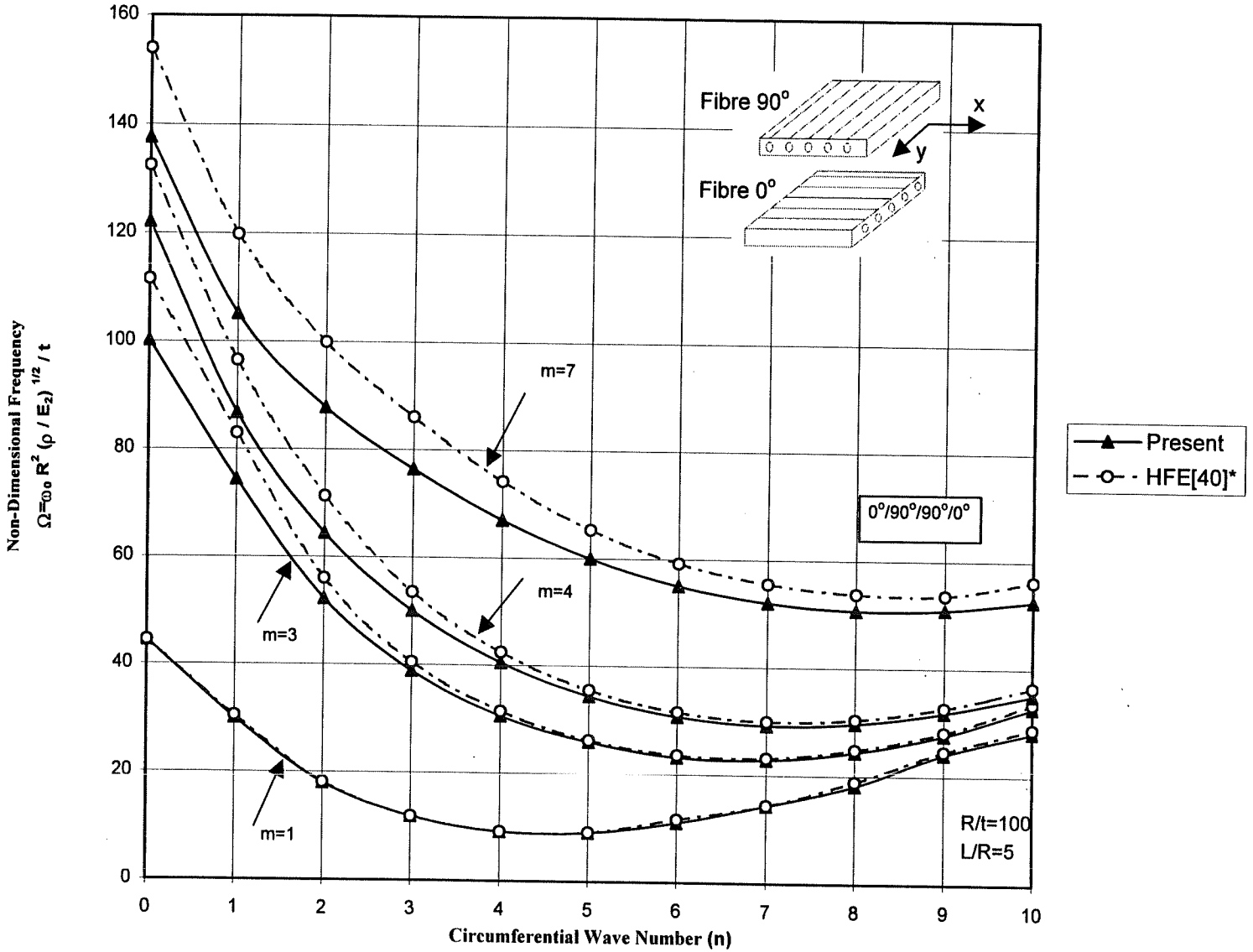

*Hybrid Finite Element Method. These results were obtained by authors.

Figure 7:Frequency distribution for various axial wave number (m) for an anisotropic cylindre

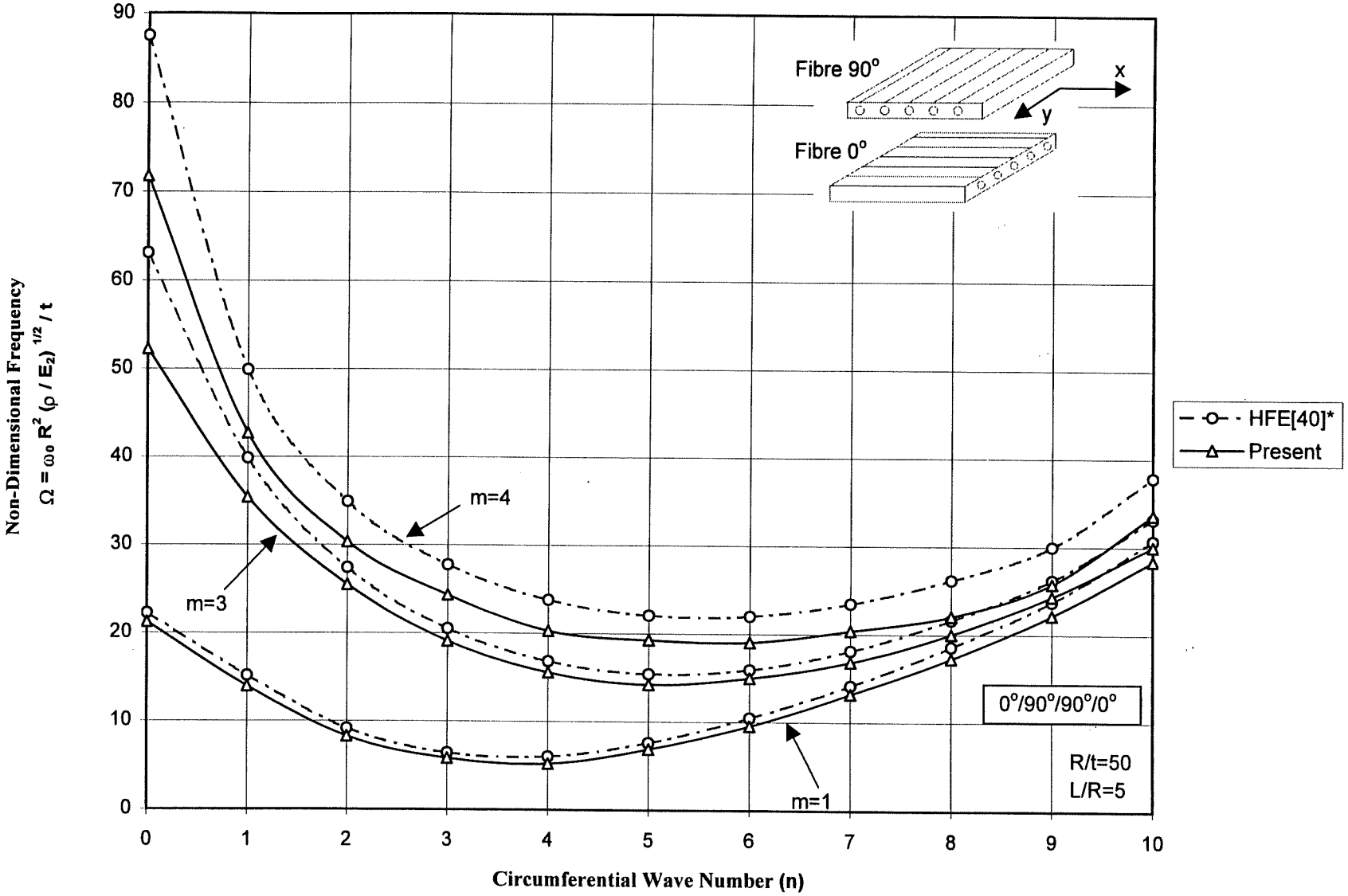

*Hybrid Finite Element Method. These results were obtained by authors.

Figure 8: Variation of non-dimensional natural frequencies in conjunction with variation of (**m**)

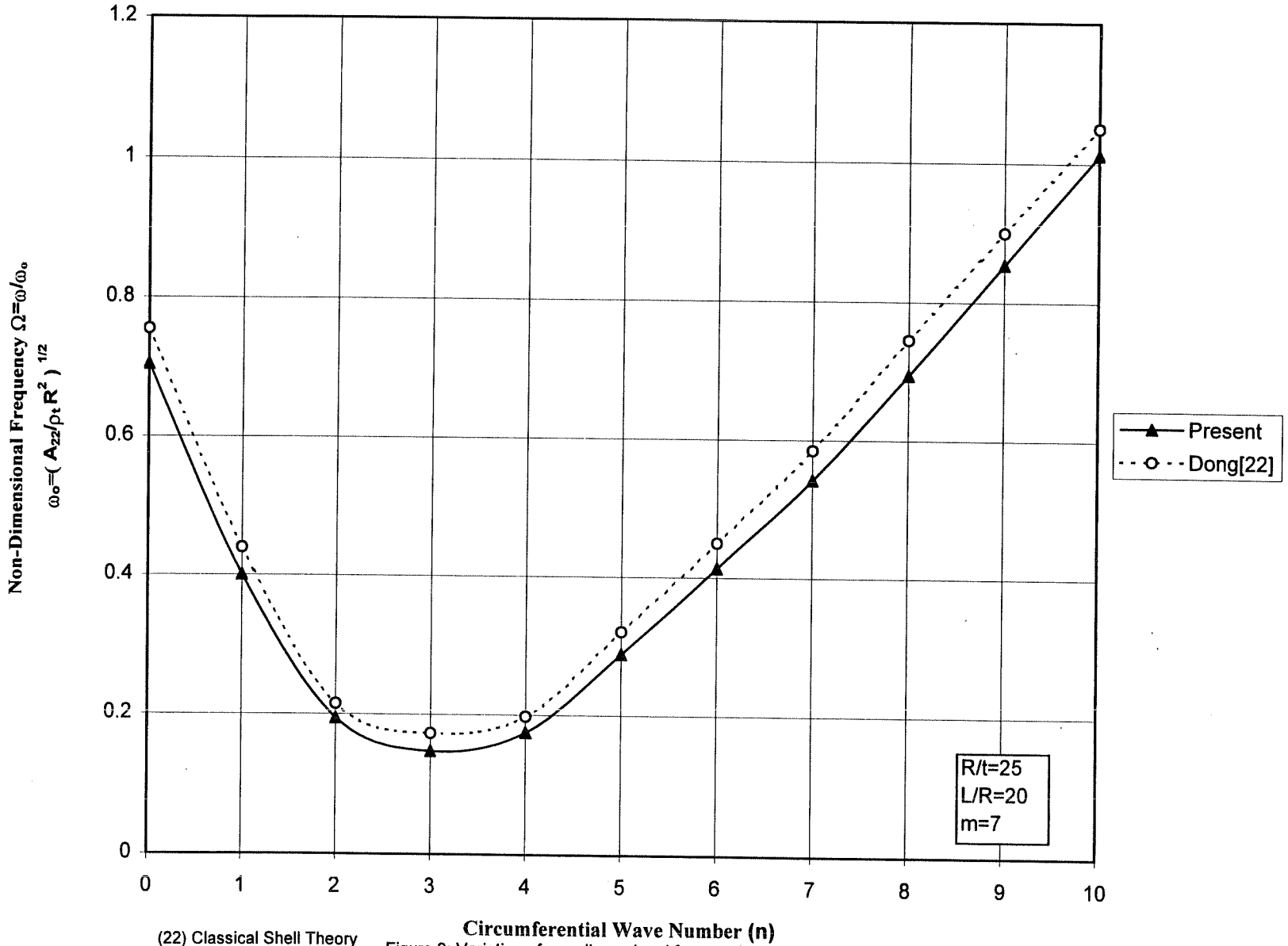

Figure 9: Variation of non-dimensional frequencies in terms of the (n) variation (m=7)

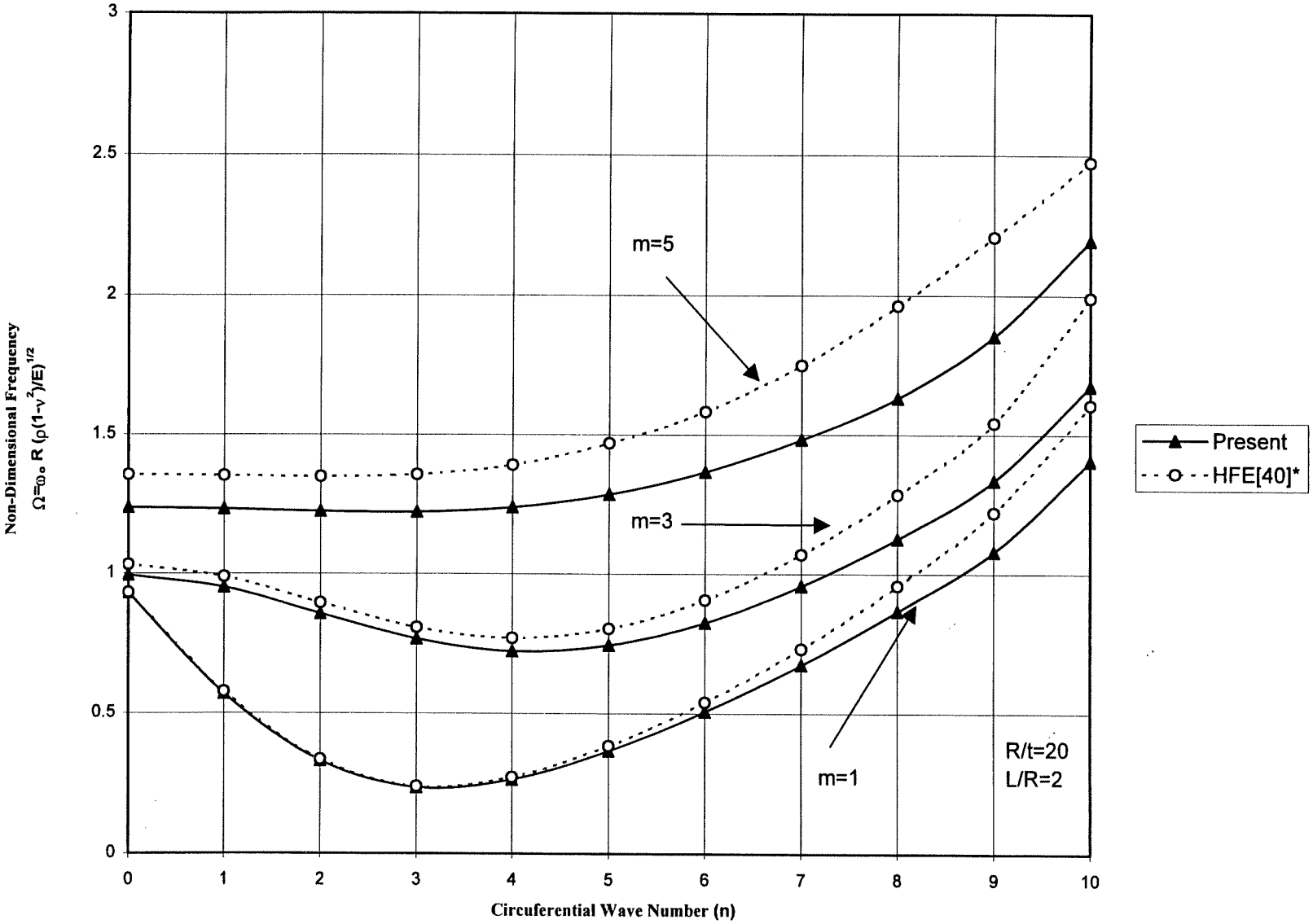

*Hybrid Finite Element Method. These results were obtained by authors.

Figure 10: Variation of non-dimensional natural frequencies in terms of the circumferential and axial mode numbers (n,m)

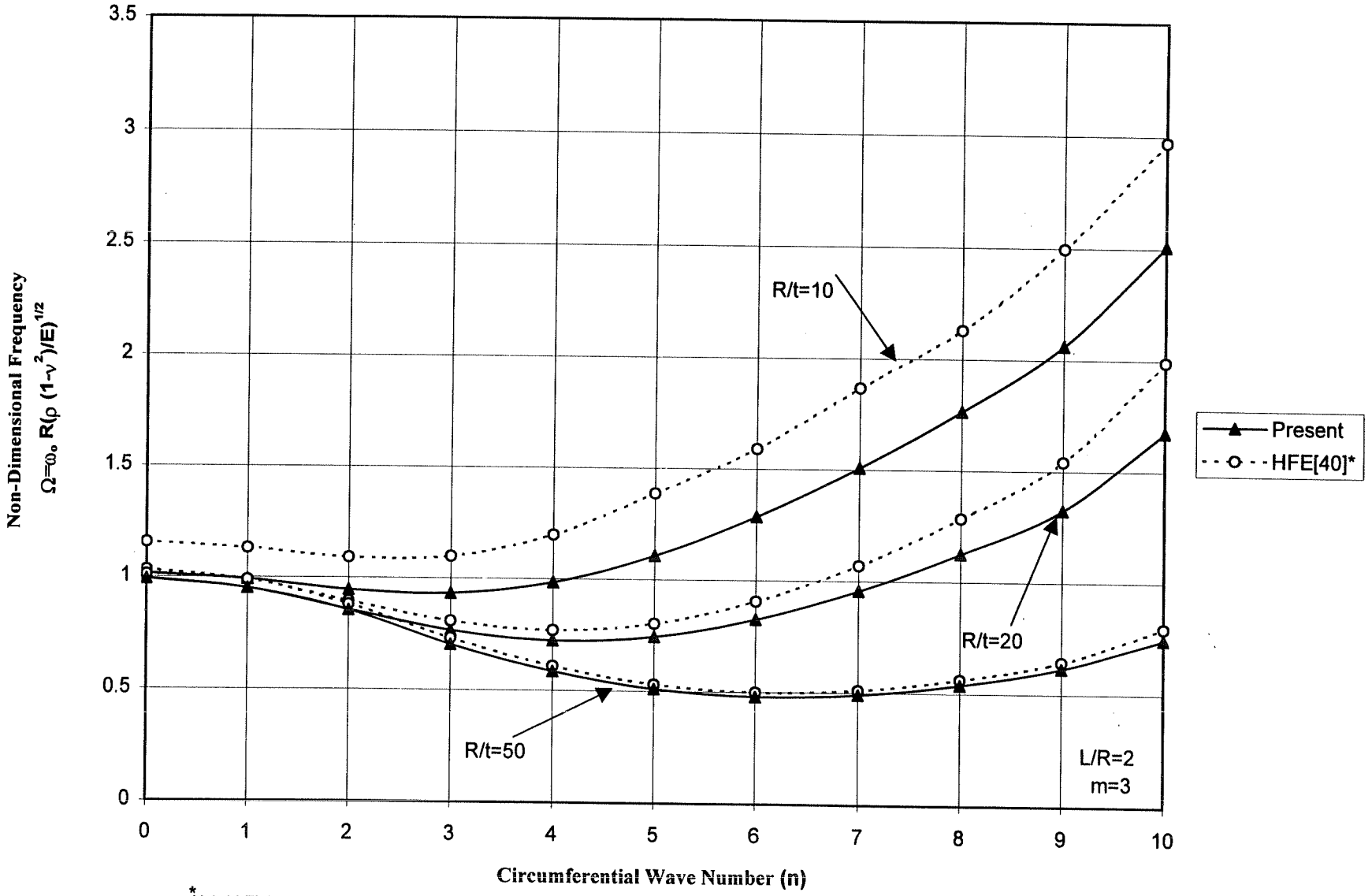

*Hybrid Finite Element Method. These results were obtained by authors.

Figure 11: Variation of non-dimensional natural frequencies in terms of the (n) and R/t

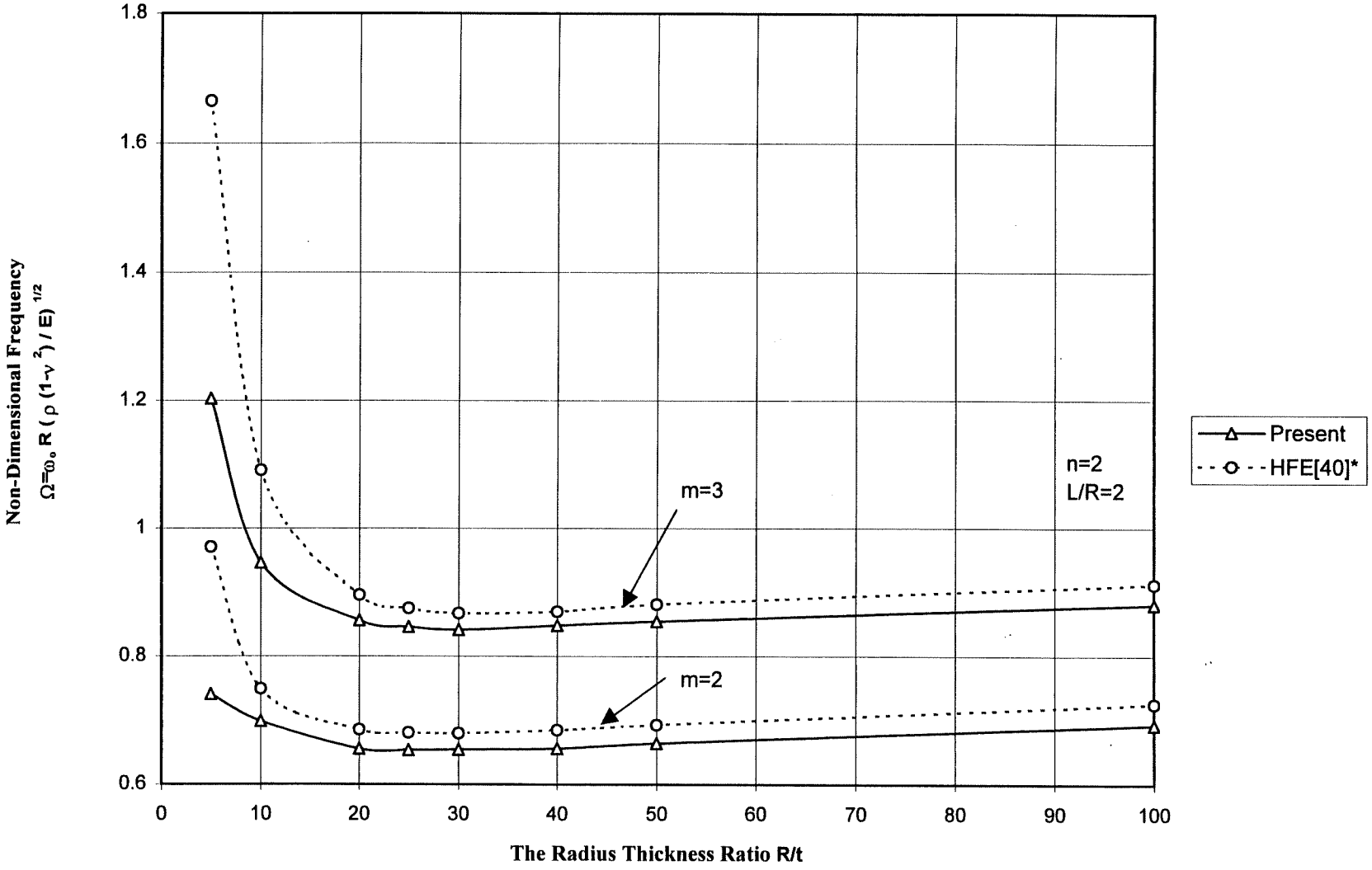

*Hybrid Finite Element Method. These results were obtained by authors.

Figure 12: Variation of non-dimensional natural frequencies in conjunction with **R/t** and **(m)** variations(isotropic materials).

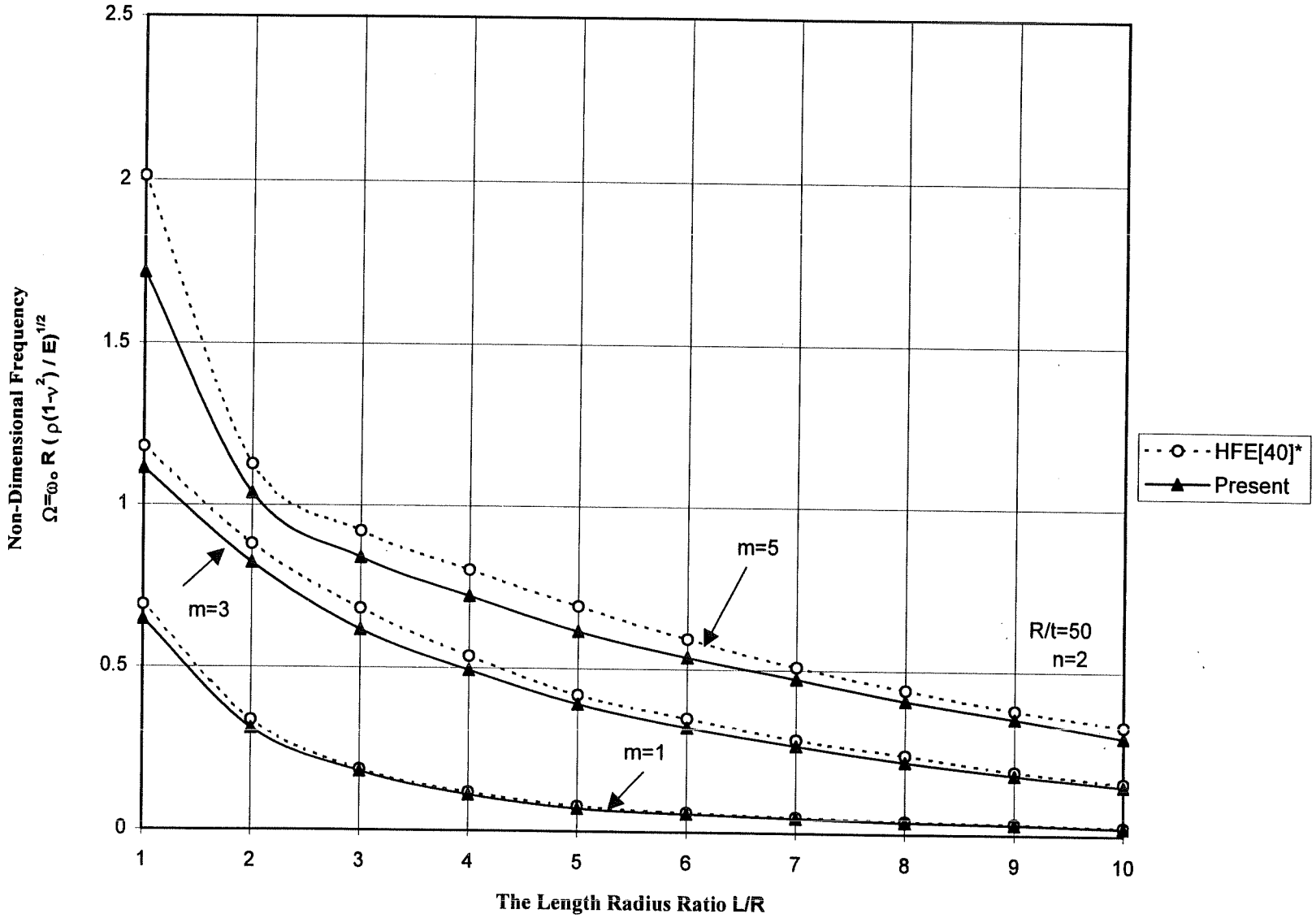

*Hybrid Finite Element Method. These results were obtained by authors.

Figure 13: Variation of non-dimensional natural frequencies in terms of L/R and (m) variations.

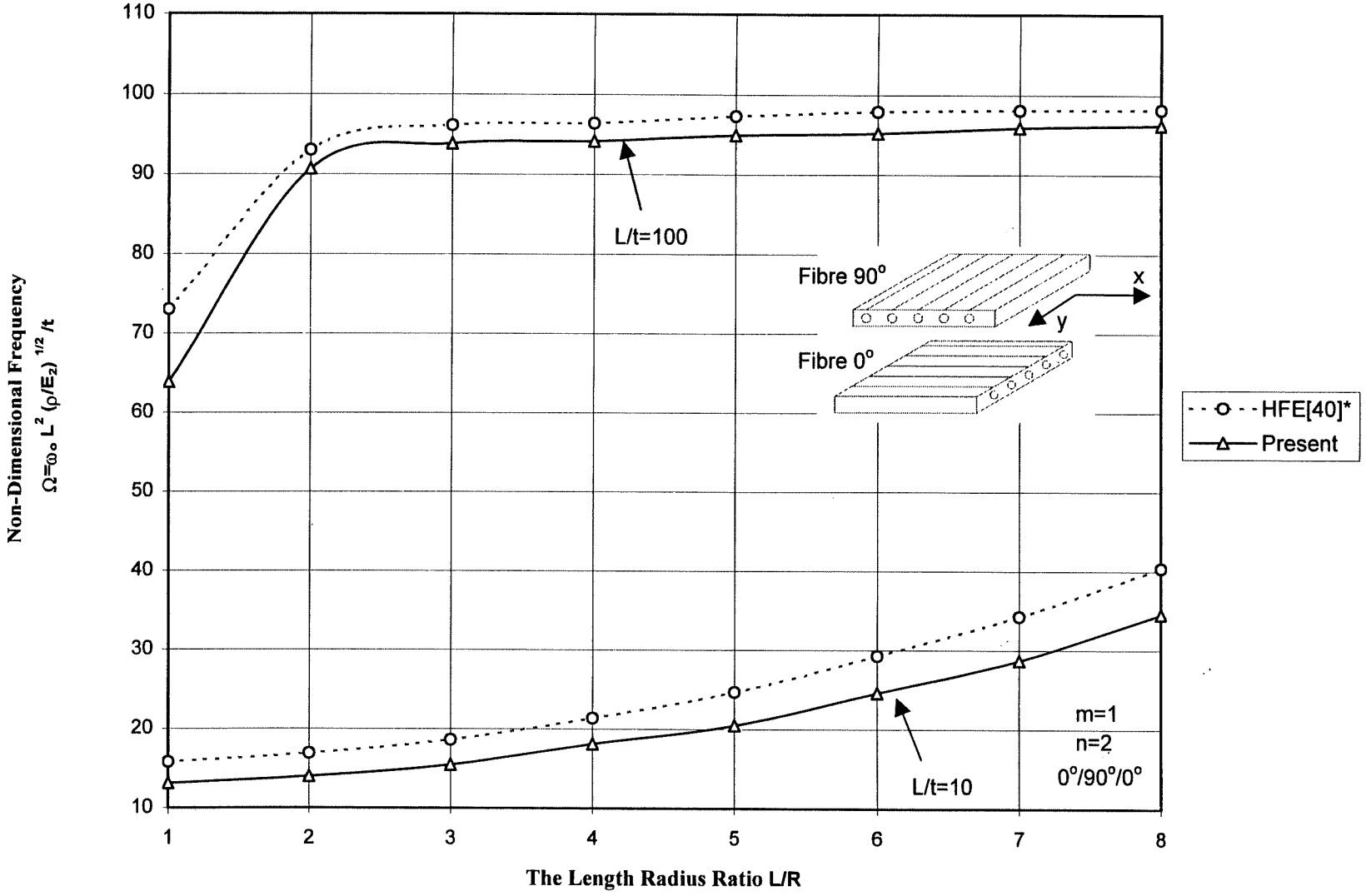

*Hybrid Finite Element Method. These results were obtained by authors.

Figure 14: The effect of the length to thickness ratio on the non-dimensional frequencies of three layered anisotropic cylindrical shells.

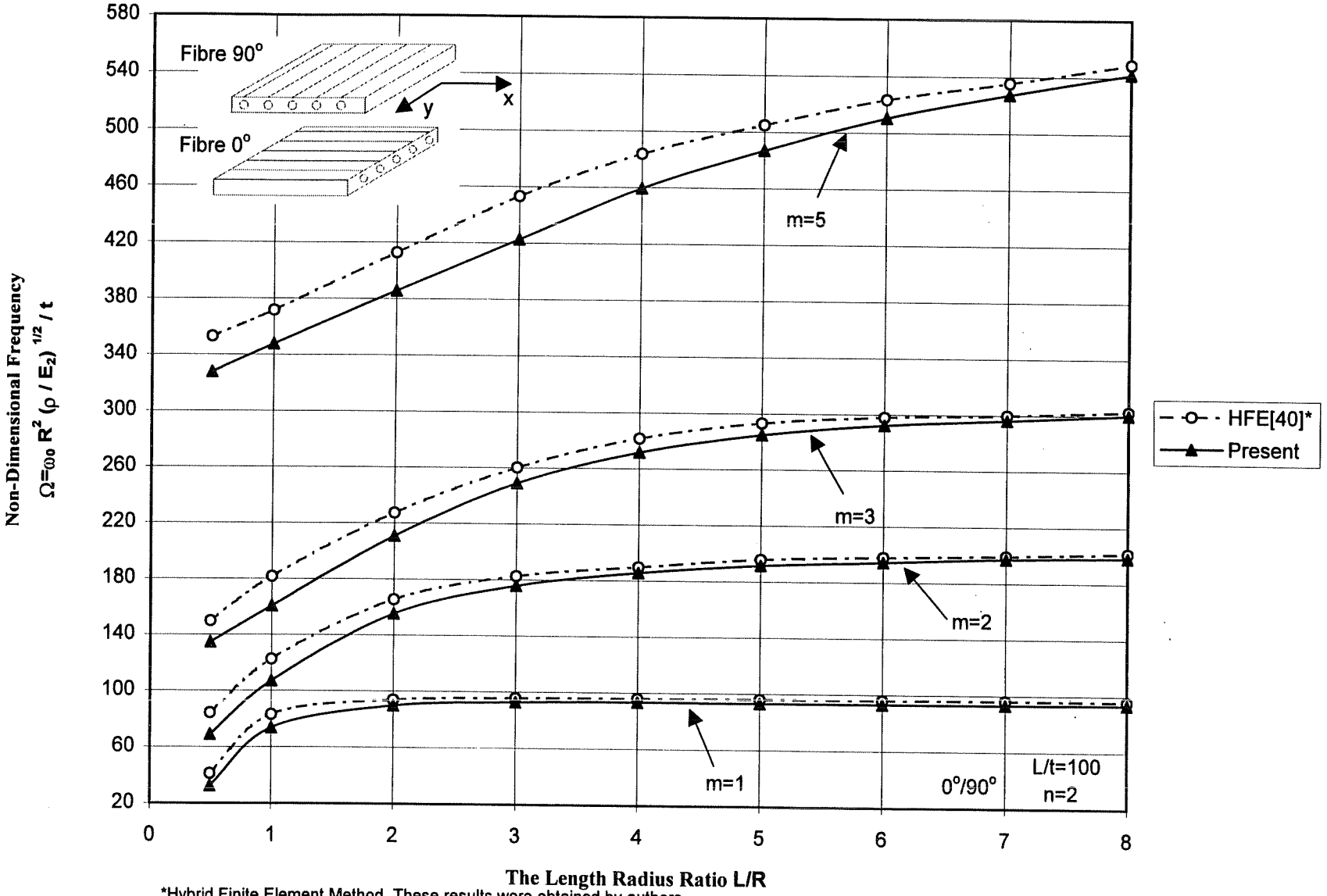

*Hybrid Finite Element Method. These results were obtained by authors.

Figure 15: Variation of non-dimensional natural frequencies of anti-symmetric cross-ply lamniated cylindrical shells in conjunction with L/R and (m) varitions.

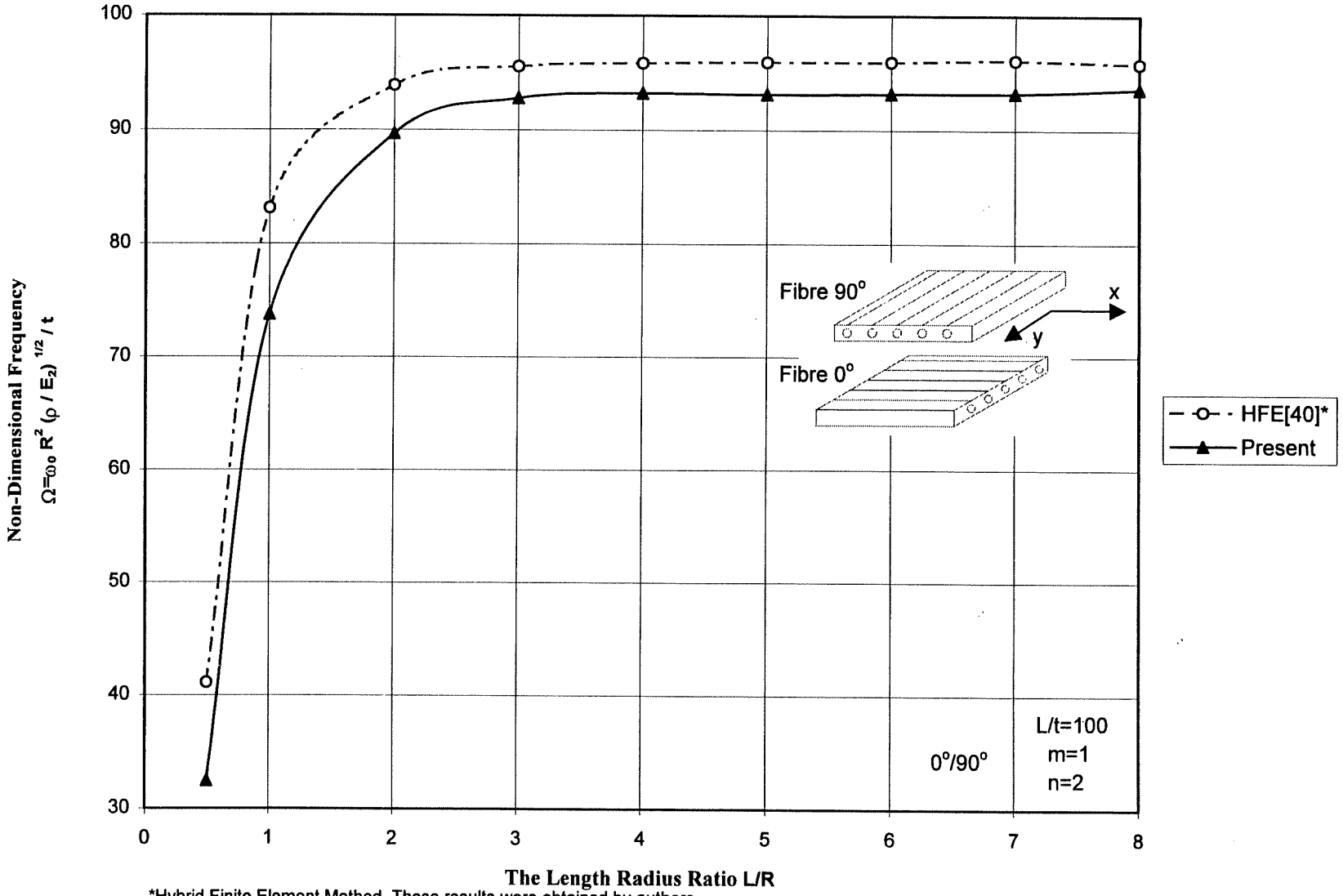

*Hybrid Finite Element Method. These results were obtained by authors.

Figure 16: Variation of non-dimensional frequencies of cross-ply cylindrical shells in terms of the L/R's variations.

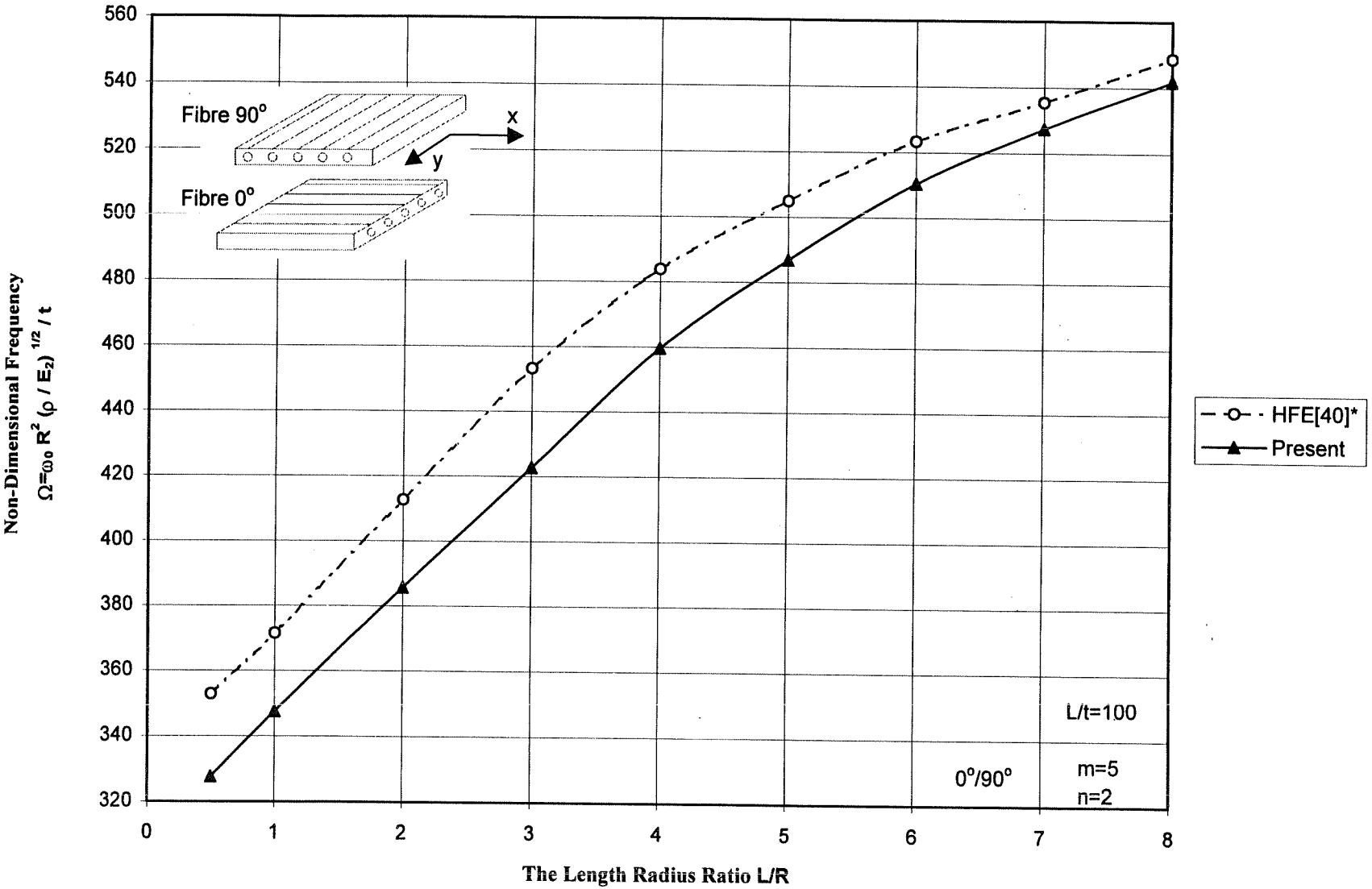

*Hybrid Finite Element Method. These results were obtained by authors.

Figure 17: Variation of non-dimensional frequencies of cross-ply cylindrical shells in terms of the L/R's variations.

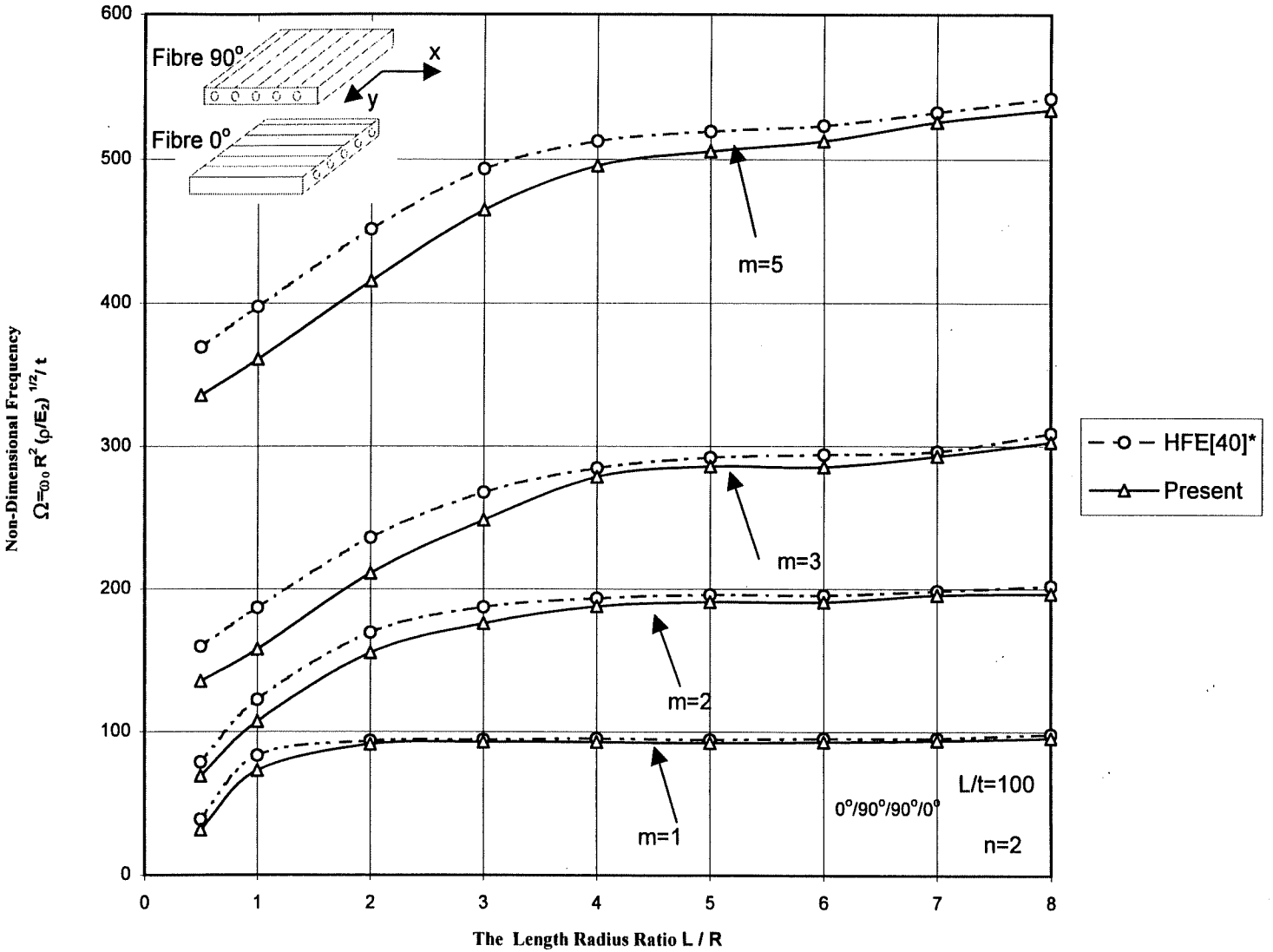

*Hybrid Finite Element Method. These results were obtained by authors.

Figure 18: Frequency distribution for various axial mode number of symmetric cross-ply laminated cylindrical shells.

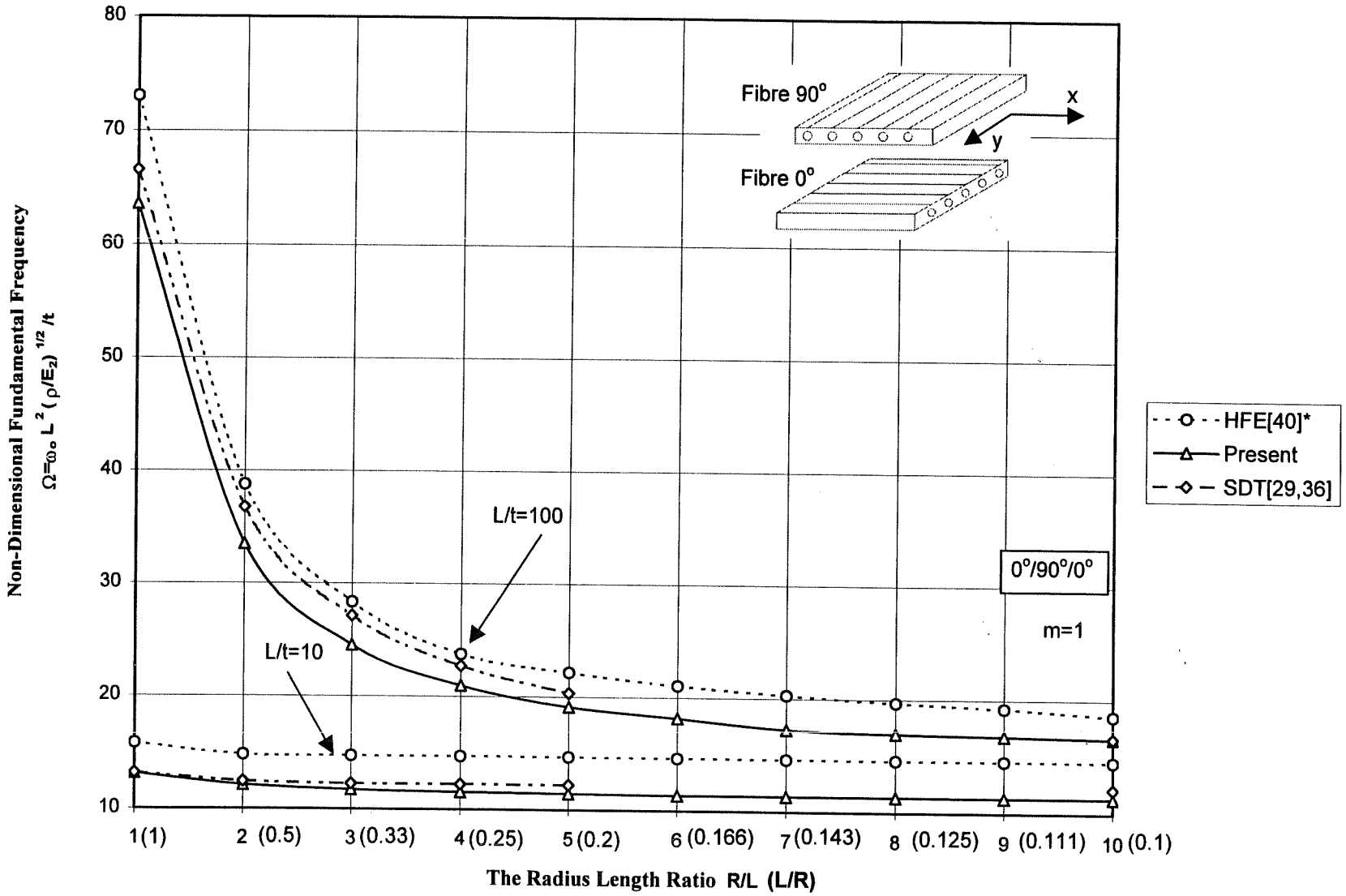

*Hybrid Finite Element Method. SDT:Shear Deformation Theory

Figure 19: Variation of non-dimensional frequency of cross-ply laminated cylindrical shell in conjunction with L/R and L/t variations.

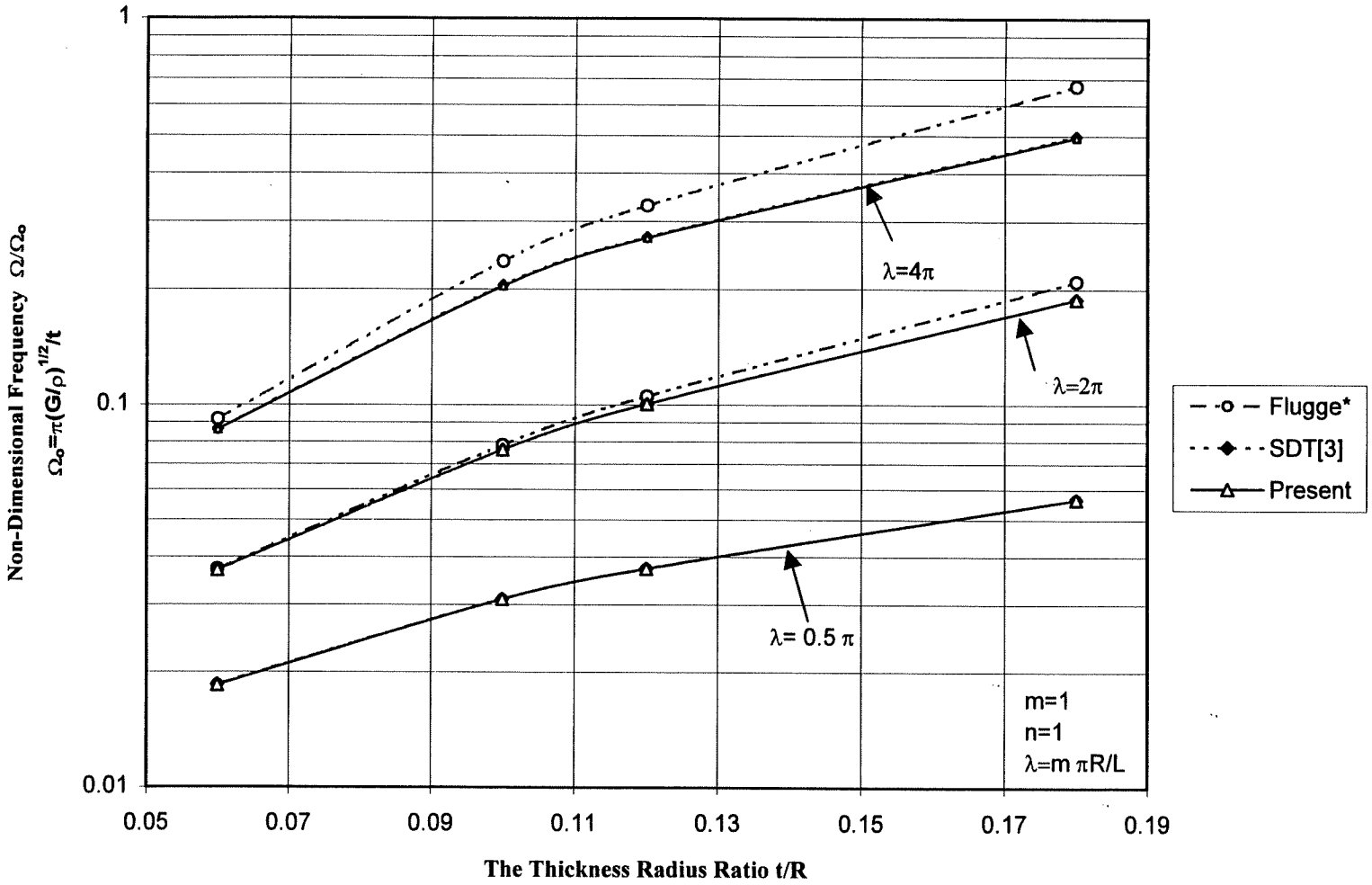

* Ref.3, SDT: Shear Deformation Theory

Figure 20: Frequency distribution for various axial mode number in terms of **t/R**'s variation

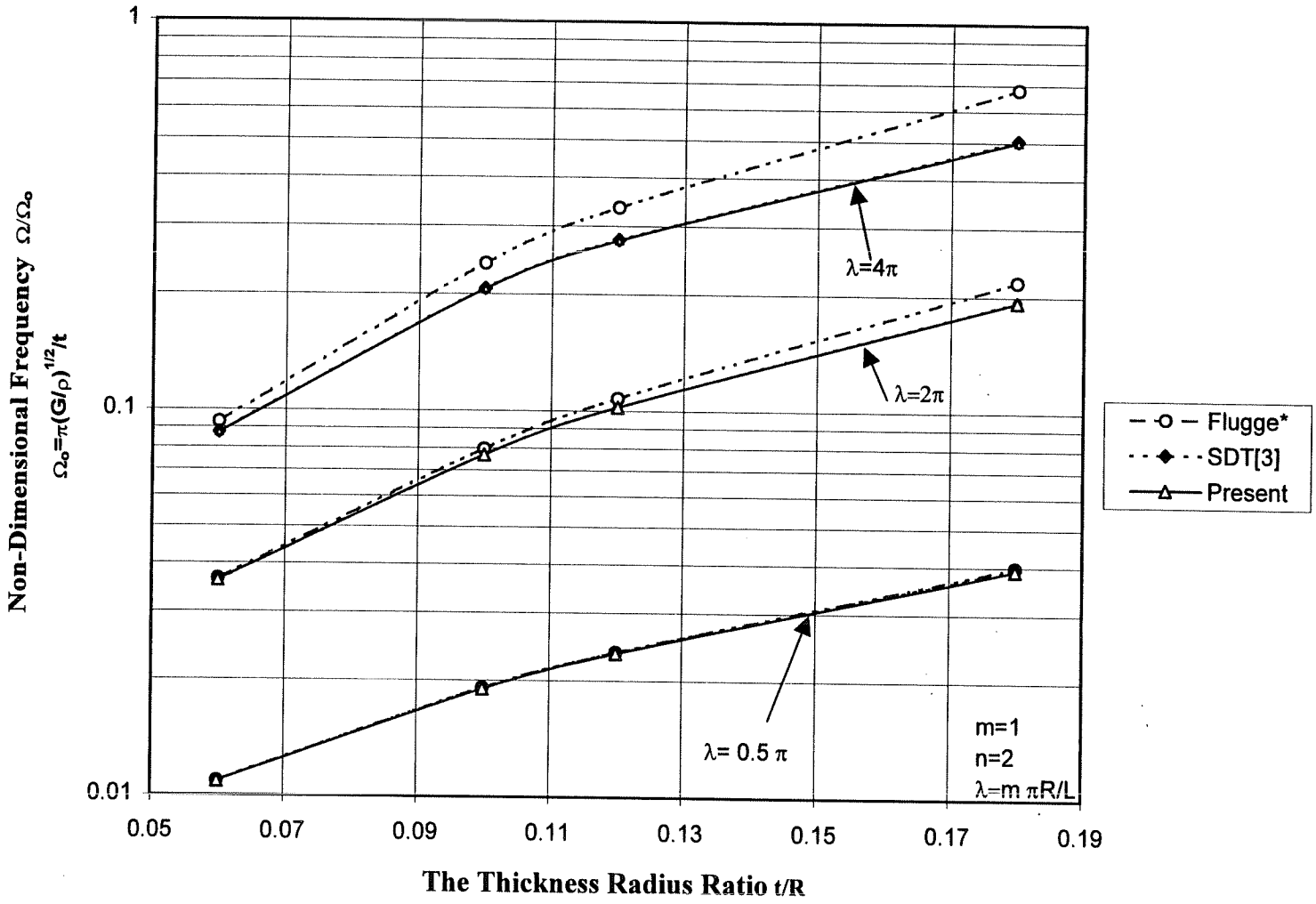

SDT: Shear Deformation Theory

Figure 21: Frequency distribution for various axial mode number in terms of t/R's variation

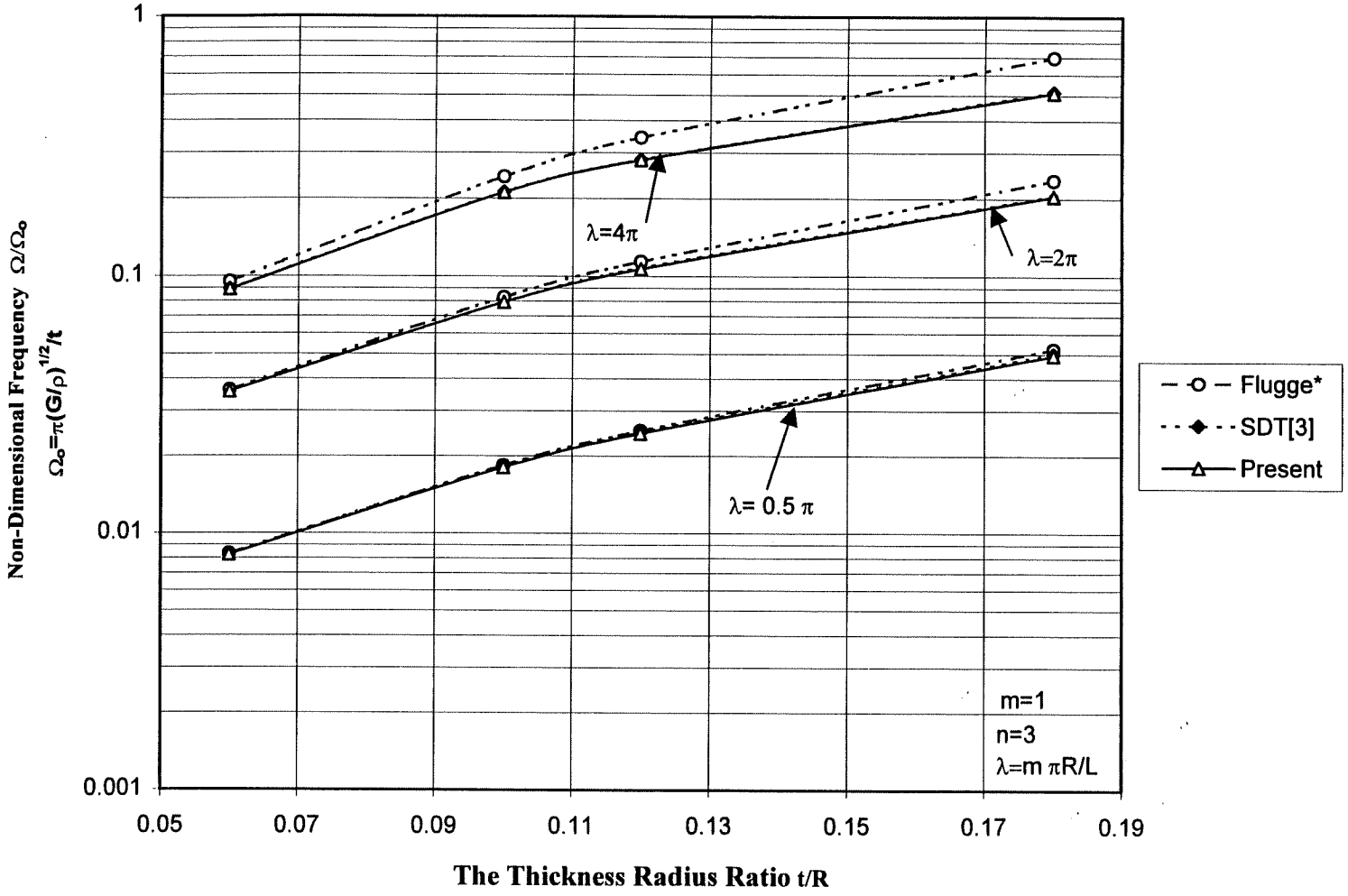

* Ref.3,SDT:Shear Deformation Theory

Figure 22:Frequency distribution for various axial mode number in terms of t/R's variation.

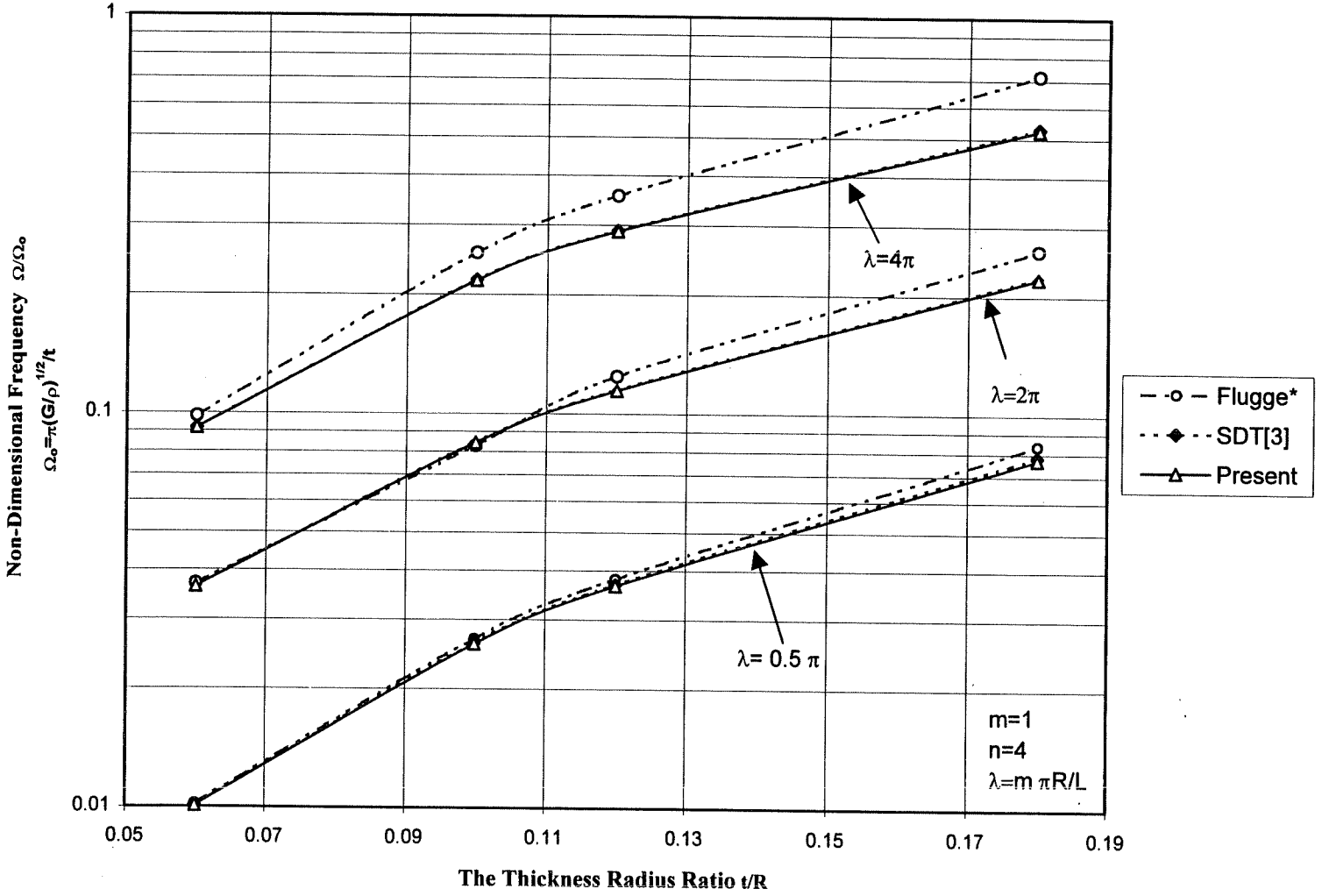

*Ref.3 , SDT:Shear Deformation Theory

Figure 23: Frequency distribution for various axial mode number in terms of t/R's variation.

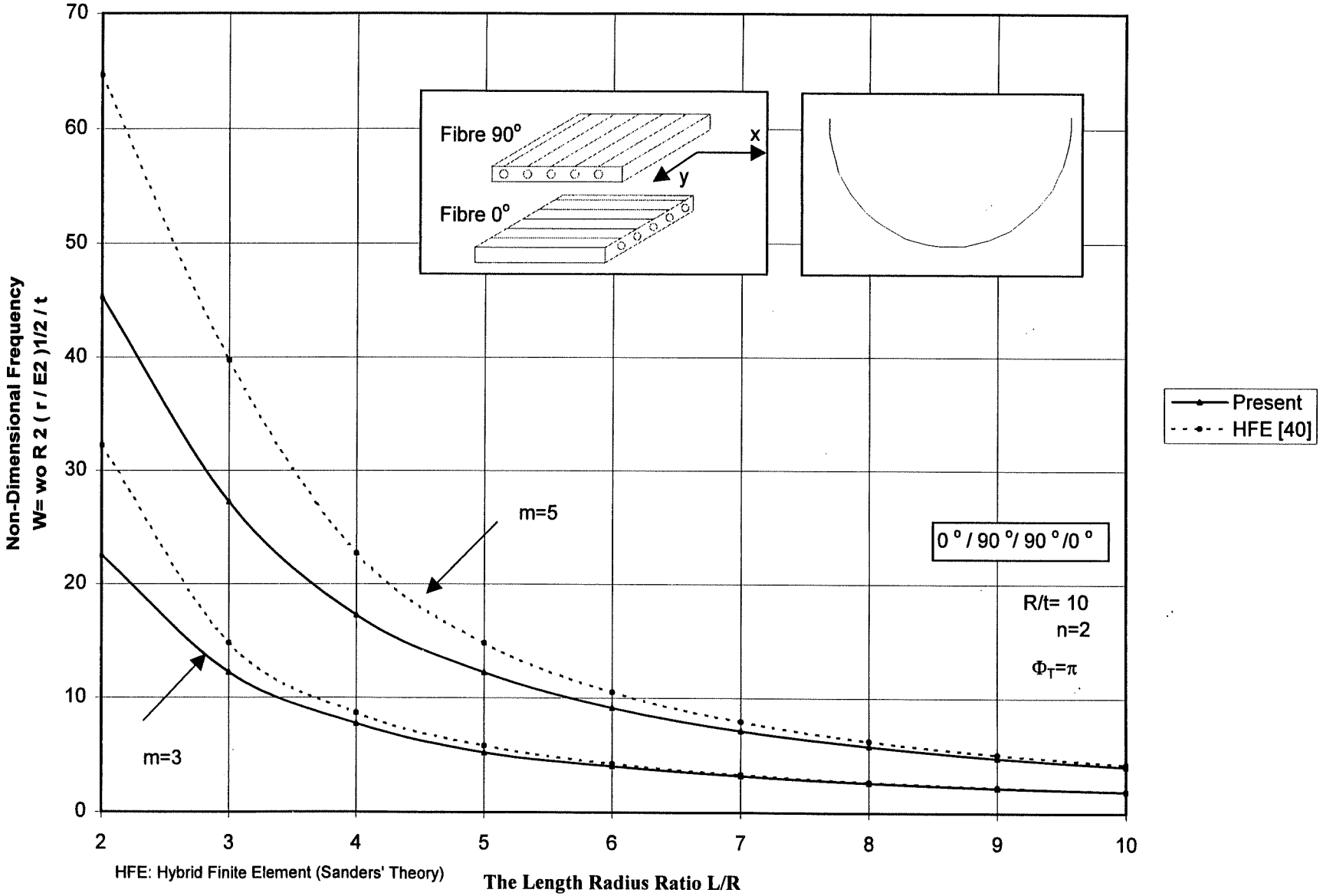

Figure 24: Variation of non-dimensional natural frequency of a cross-ply open cylindrical shell for various of **L/R** and **m**.

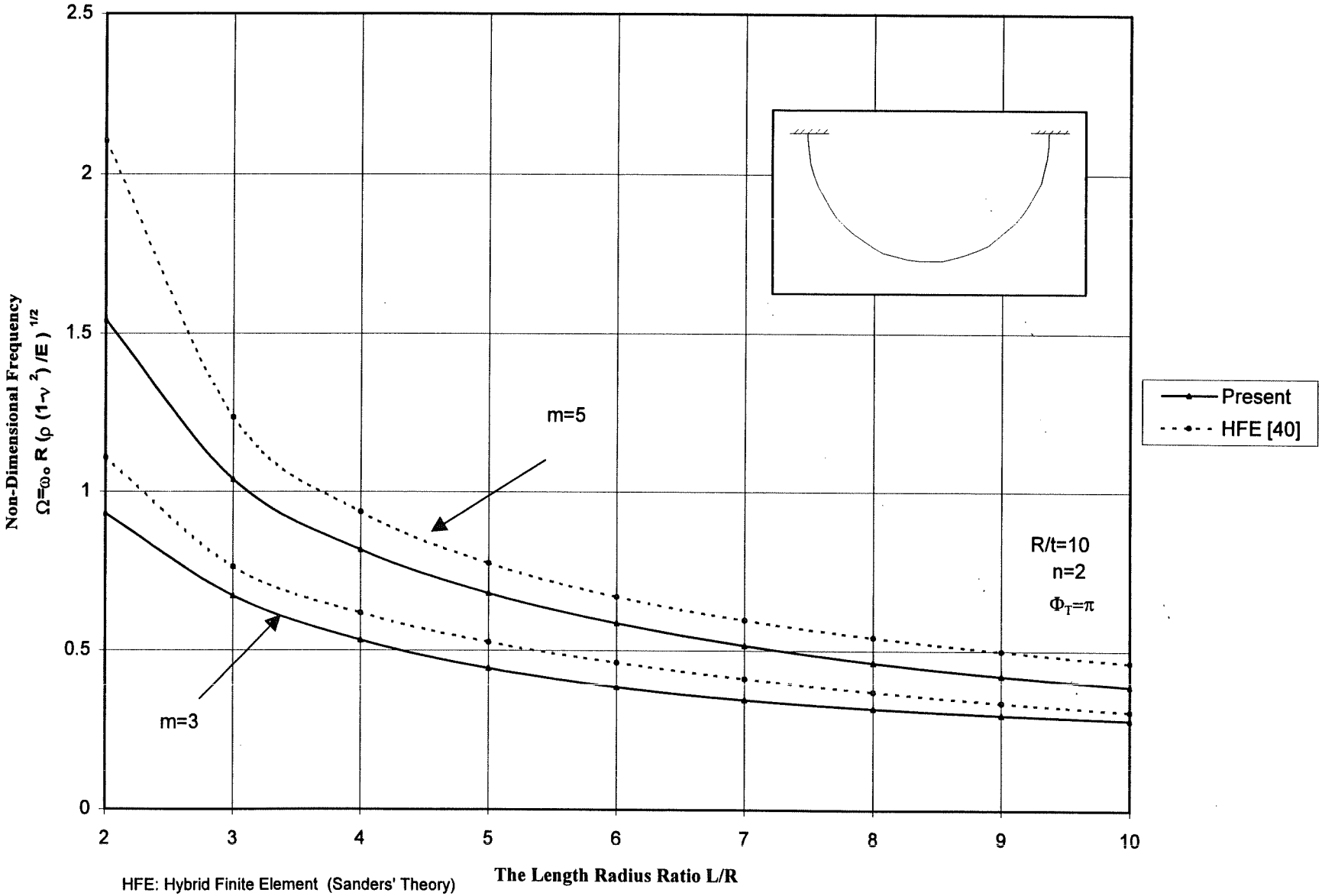

HFE: Hybrid Finite Element (Sanders' Theory)

Figure 25:Frequency distribution of an open cylindrical shell in conjunction with **L/R** and **m** variations.